

A Scotogenic Model as a Prototype for Leptogenesis with One Single Gauge Singlet

Björn Garbrecht^a and Edward Wang^b

*Physik-Department T70, Technische Universität München,
James-Frank-Straße, 85748 Garching, Germany*

We investigate the potential of a minimal Scotogenic model with two additional scalar doublets and a single heavy Majorana fermion to explain neutrino masses, dark matter, and the baryon asymmetry of the Universe. In this minimal setup, Leptogenesis is purely flavored, and a second Majorana neutrino is not necessary because the Yukawa couplings of the extra doublets yield the necessary CP -odd phases. The mechanism we employ can also be applied to a wide range of scenarios with at least one singlet and two gauge multiplets. Despite stringent limits from the dark matter abundance, direct detection experiments, and the baryon asymmetry of the Universe, we find a parametric region consistent with all bounds which could resolve the above shortcomings of the Standard Model of particle physics. Methodically, we improve on the calculation of correlations between the mixing scalar fields given their finite width. We also present an argument to justify the kinetic equilibrium approximation for out-of-equilibrium distribution functions often used in calculations of Baryogenesis and Leptogenesis.

I. Introduction

Leptogenesis is a possible explanation of the baryon asymmetry of the universe (BAU) motivated by neutrino mass mechanisms. In the type-I seesaw mechanism, left-handed neutrinos couple to at least two heavy Majorana fermions through the Standard Model (SM) Higgs doublet, so that at least two neutrinos become massive. The interferences between amplitudes involving the different Majorana fermions give rise to CP -odd phases in their decays [1]. The asymmetry arising from these CP -violating decays is first produced in the leptons and subsequently transferred to the baryon sector via sphaleron transitions. In the present work we explore an alternative mechanism, in which CP -violation arises from interferences of amplitudes involving different multiplets of the SM gauge group instead of singlets, building upon previous work in Refs. [2, 3]. A singlet however still induces the necessary deviation from equilibrium, but for this sole purpose, just a single one is sufficient. When the multiplets taking part in the interferences do not have lepton number violating interactions, Leptogenesis is purely flavored, i.e., the net sum of the decay and inverse decay asymmetries over the flavors is zero. Nonvanishing symmetries in the particular flavors lead to a net unflavored asymmetry through washout processes involving the singlet. Minimal scenarios therefore consist of one singlet and at least two multiplets leading to mixing and interference, and the latter must couple to at least two different flavors of SM fermions.

The interferences between amplitudes involving the different multiplets can then lead to an asymmetry in the decay of the heaviest particle, which can be either the singlet or one of the multiplets. In both cases, it is the singlet that drives the system out of equilibrium. Since the multiplets participate in the SM gauge interactions, they tend to equilibrate quickly and through processes that do not involve asymmetry production, whereas the singlet can only equilibrate via its interactions with the multiplets, where CP -violation occurs. The diagrams for the relevant tree and loop amplitudes are shown in Figure 1, where S stands for the singlet and $\chi_{a,b}$ are the multiplets.

In order to preserve gauge invariance, the multiplets must have the same quantum numbers as the SM fermions to which they couple with the singlet at the renormalizable level. Examples of models containing additional $SU(2)_L$ doublets that can generally lead to CP -violating interferences are Scotogenic models [4–13], two-Higgs-doublet models [14–35], and inert doublet models [36–45], and aim at addressing such problems as dark matter, neutrino masses, muon $g - 2$, among others. Models containing additional scalar color triplets have also been proposed [46–49] and are a common prediction of Grand Unified Theories, although there the mass of the triplet has to be very large to avoid proton decay, leading to the doublet-triplet mass splitting problem [50–53]. Another possibility would be to have interferences involving sfermions or Higgsinos in supersymmetric models, which by construction have the same quantum numbers as their superpartners [54–69]. The mechanism we lay out in the present work can by and large be applied to these

^a garbrecht@tum.de

^b edward.wang@tum.de

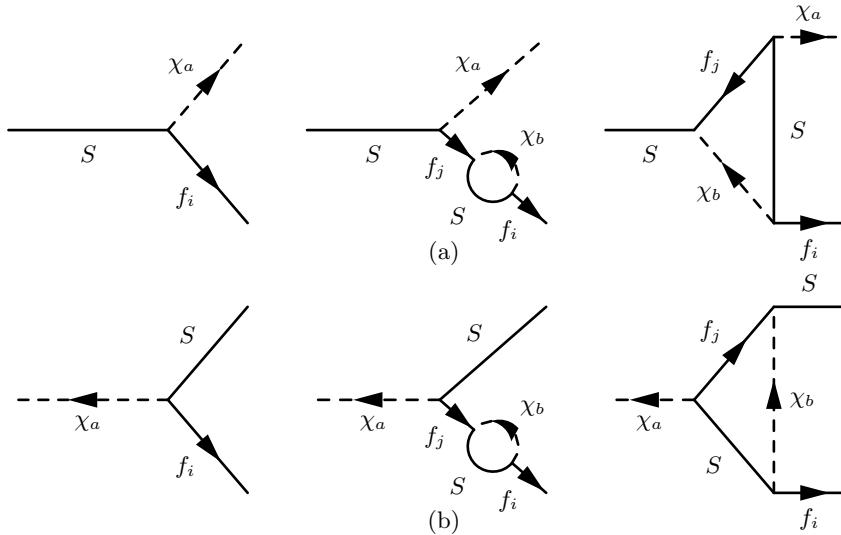


Figure 1: Tree-level, wavefunction and vertex-type contributions to decays in the case of (a) singlet and (b) multiplet decay in a general class of models, where $f_{i,j}$ are SM fermions, S is a singlet and $\chi_{a,b}$ are multiplets of the SM gauge group. While the dashed and solid lines typically represent scalars and fermions respectively, exchanging the fermionic/bosonic natures of χ and S is also possible.

scenarios, when one or more multiplets mix and interfere to produce CP -violating interactions. While in the remainder of this work we will consider the usual case of a fermionic singlet and a scalar multiplet, the opposite case is also possible.

In the present work, we demonstrate how this general mechanism applies to a minimal variant of the Scotogenic model. Scotogenic models are a class of Beyond the Standard Model (BSM) scenarios aiming to explain the smallness of neutrino masses while also including a dark matter (DM) candidate. The original Scotogenic model [70] extends the SM by a dark sector, odd under a new \mathbb{Z}_2 symmetry and containing one extra Higgs doublet and two Majorana fermions. Due to the \mathbb{Z}_2 symmetry, the lightest particle of this new sector is absolutely stable and therefore a dark matter candidate. Soon after its proposal, it was realized that the Scotogenic model also has the potential for producing Leptogenesis in a similar way as in the Seesaw model [71].

Several variants of the original model have been put forward and studied extensively. The model we investigate here was proposed in Ref. [72] and is an alternative minimal realization of the Scotogenic model, with two additional scalar doublets instead of one and only a single Majorana fermion. The goal of this work, in addition to the above considerations, is to explore the possibility of explaining neutrino masses, the baryon asymmetry of the universe, and dark matter in this minimal scenario. Similar attempts, based on other variants of the Scotogenic model, have been reported in Refs. [73–78].

The outline of the article is as follows: In Section II we present the model and its properties, in Section III we discuss some of the main constraints of the model and in Section IV we present the details of our calculation of Leptogenesis. In Section V we discuss the dark matter production in our model and in Section VI we present the allowed parameter region.

II. The Model

The model we consider was proposed in Ref. [72] and extends the Standard Model by one Majorana fermion N and two complex scalars $\eta_{1,2}$, doublets under $SU(2)_L$ and with hypercharge $1/2$. Furthermore, a discrete \mathbb{Z}_2 symmetry is imposed under which the Standard Model particles are even, while the new particles are odd. The Lagrangian for this model is given by

$$\mathcal{L} = \mathcal{L}_{\text{SM}} + \mathcal{L}_N + \mathcal{L}_\eta + \mathcal{L}_{\text{int}}^{\text{fermion}} + \mathcal{L}_{\text{int}}^{\text{scalar}}, \quad (1)$$

where \mathcal{L}_{SM} is the SM Lagrangian. The Scotogenic sector is introduced through

$$\mathcal{L}_N = \frac{1}{2} \bar{N}^c i \not{\partial} N - \frac{1}{2} M_N \bar{N}^c N + \text{h.c.}, \quad (2)$$

$$\mathcal{L}_\eta = (D_\mu \eta^a)^\dagger (D^\mu \eta_a) - (m_\eta^2)_{ab} \eta^{a\dagger} \eta^b - V(\eta_1, \eta_2), \quad (3)$$

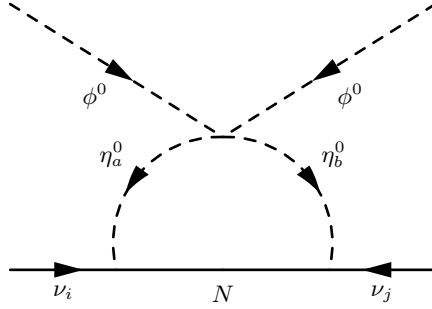


Figure 2: Diagram generating neutrino masses in this model.

where D_μ is the covariant derivative and $V(\eta_1, \eta_2)$ is the general potential of a two-Higgs doublet model. We can define the mass matrix $(m_\eta^2)_{ab}$ to be diagonal, with values $m_{\eta_1}^2$ and $m_{\eta_2}^2$. Interactions between the SM and Scotogenic sector are given by

$$\mathcal{L}_{\text{int}}^{\text{fermion}} = -Y_i^{(a)} \bar{N} (L_i i \sigma_2 \eta_a) + \text{h.c.} = -Y_i^{(a)} \bar{N} (\nu_i \eta_a^0 - l_i^- \eta_a^+) + \text{h.c.}, \quad (4)$$

$$\mathcal{L}_{\text{int}}^{\text{scalar}} = -\frac{1}{2} \lambda_3^{(ab)} (\Phi^\dagger \Phi) (\eta_a^\dagger \eta_b) - \frac{1}{2} \lambda_4^{(ab)} (\Phi^\dagger \eta_a) (\eta_b^\dagger \Phi) - \frac{1}{2} \lambda_5^{(ab)} (\Phi^\dagger \eta_a) (\Phi^\dagger \eta_b) + \text{h.c.}, \quad (5)$$

where h.c. stands for Hermitian conjugation. We assume the discrete symmetry \mathbb{Z}_2 to remain unbroken, meaning that the fields η_1 and η_2 do not acquire a vacuum expectation value, whereas for the SM Higgs field Φ we have $\langle \Phi^0 \rangle = v/\sqrt{2}$.

The left-handed neutrinos do not directly couple to the SM Higgs field and therefore cannot obtain mass at tree level. The leading contribution to the mass at one-loop order shown in Figure 2 is

$$(m_\nu)_{ij} = \frac{Y_i^{(a)} Y_j^{(b)} \lambda_5^{(ab)} v^2}{8\pi^2} \frac{M_N}{m_{\eta_b}^2 - M_N^2} \left(\frac{m_{\eta_b}^2}{m_{\eta_a}^2 - m_{\eta_b}^2} \log \left(\frac{m_{\eta_a}^2}{m_{\eta_b}^2} \right) - \frac{M_N^2}{m_{\eta_a}^2 - M_N^2} \log \left(\frac{m_{\eta_a}^2}{M_N^2} \right) \right), \quad (6)$$

where we sum over $a, b = 1, 2$. Neutrino masses are then expected to be small if the couplings Y and λ_5 are small or if the heaviest mass scale is much above the electroweak scale. In principle, different hierarchies of the masses of the new dark particles are possible; we will, however, restrict ourselves to the scenario in which

$$m_{\eta_2} > M_N > m_{\eta_1}. \quad (7)$$

After electroweak symmetry breaking, the coupling of the new scalars to the SM Higgs field gives a correction to their masses. We can parametrize the scalar fields as

$$\eta_a = \begin{pmatrix} \eta_a^+ \\ \eta_a^0 \end{pmatrix} = \begin{pmatrix} \eta_a^+ \\ \frac{1}{\sqrt{2}} (\eta_{Ra} + i \eta_{Ia}) \end{pmatrix}, \quad (8)$$

where η_a^+ is a charged scalar and η_{Ra} and η_{Ia} are CP even and odd neutral real scalars, respectively. The new mass matrices accounting for the vacuum expectation value are

$$(m_+^2)_{ab} = (m_\eta^2)_{aa} \delta_{ab} + \lambda_3^{ab} \frac{v^2}{2}, \quad (9)$$

$$(m_R^2)_{ab} = (m_\eta^2)_{aa} \delta_{ab} + \text{Re}(\lambda_3^{ab} + \lambda_4^{ab} + \lambda_5^{ab}) \frac{v^2}{2}, \quad (10)$$

$$(m_I^2)_{ab} = (m_\eta^2)_{aa} \delta_{ab} + \text{Re}(\lambda_3^{ab} + \lambda_4^{ab} - \lambda_5^{ab}) \frac{v^2}{2}. \quad (11)$$

In general, we assume these corrections $\sim \lambda v^2$ to be small compared to m_η^2 . With this assumption, we can approximate the mass matrices as diagonal with eigenvalues m_{Ra}, m_{Ia} . The mass splitting between the neutral scalars of a doublet is then given by [6]

$$m_{Ra}^2 - m_{Ia}^2 = \text{Re}(\lambda_5^{aa}) v^2, \quad (12)$$

with corrections appearing at second order in λv^2 .

Process	BR upper bound
$\mu^- \rightarrow e^- \gamma$	4.2×10^{-13}
$\tau^- \rightarrow e^- \gamma$	3.3×10^{-8}
$\tau^- \rightarrow \mu^- \gamma$	4.2×10^{-8}
$\mu^- \rightarrow e^- e^+ e^-$	1.0×10^{-12}
$\tau^- \rightarrow e^- e^+ e^-$	2.7×10^{-8}
$\tau^- \rightarrow \mu^- \mu^+ \mu^-$	2.7×10^{-8}

Table 1: LFV processes and their respective upper bounds, extracted from Ref. [80].

III. Constraints

A. Lepton Flavor Violation

Scotogenic models predict lepton flavor violating (LFV) processes such as the radiatively induced decays $\ell_i \rightarrow \ell_j \gamma$ and $\ell_\alpha \rightarrow 3\ell_\beta$. The corresponding branching ratios have been computed in Ref. [79], and the relevant upper bounds from Ref. [80] are listed in Table 1.

B. Direct detection

The couplings of the dark matter particle η_1 to the SM Higgs and to the weak gauge bosons will produce a signature in direct detection experiments. If the CP even and odd neutral components of the scalars are degenerate in mass, the spin-independent elastic cross section due to Z -boson exchange of the dark matter particle on nuclei is many orders of magnitude larger than allowed by experiments [81]. To avoid this constraint, it is necessary to have a sufficiently large mass splitting ($O(100)$ keV) between the two neutral scalars so that their kinetic energy is insufficient to upscatter in a ground-based detector. This can be achieved with sufficiently large λ_5 , as per Eq. (12).

A second detection channel is through elastic scattering via Higgs boson exchange. This sets an upper bound on the allowed values for the scalar interactions. Defining $\lambda_{345} = \lambda_3 + \lambda_4 - |\lambda_5|$ as the coupling strength between the lightest dark scalar and the SM Higgs boson, the spin-independent DM-nucleon scattering cross-section is given by

$$\sigma_{\text{SI}} = \frac{\lambda_{345}^2 f_n^2 \mu^2 m_n^2}{4\pi m_h^4 m_\eta^2}, \quad (13)$$

with $\mu = m_n m_\eta / (m_n + m_\eta)$ the DM-nucleon reduced mass, m_h the SM Higgs boson mass and $f_n \approx 0.32$ the Higgs-nucleon coupling [82]. This cross-section is then constrained by direct detection experiments like LUX-ZEPLIN [83].

C. Theoretical Constraints

There are two main theoretically motivated constraints on our model. The first comes from the requirement of perturbativity. For a perturbative treatment of the theory to be possible, the coupling strengths should not be larger than $O(1)$. This is especially important since, as we will see, an interplay between the different masses and couplings is necessary to reproduce the correct neutrino masses, leading to unacceptably large couplings in some regions of the parameter space.

The second constraint comes from vacuum stability. The situation in three-Higgs-doublet models is similar to the two-Higgs-doublet case, which is well understood [14, 84, 85], albeit somewhat more complicated. In general, however, the parameters of the scalar potential $V(\eta_1, \eta_2)$ can be chosen such that the full theory is stable. We will therefore not delve deeper into this issue, as this is not the focus of the present work. One important aspect, however, is that the dark matter candidate should be electrically neutral; this can be achieved if $\lambda_4 - |\lambda_5| < 0$, see Eqs. (9) to (11). For a more thorough discussion on vacuum stability in three-Higgs-doublet models see Refs. [15, 17, 20].

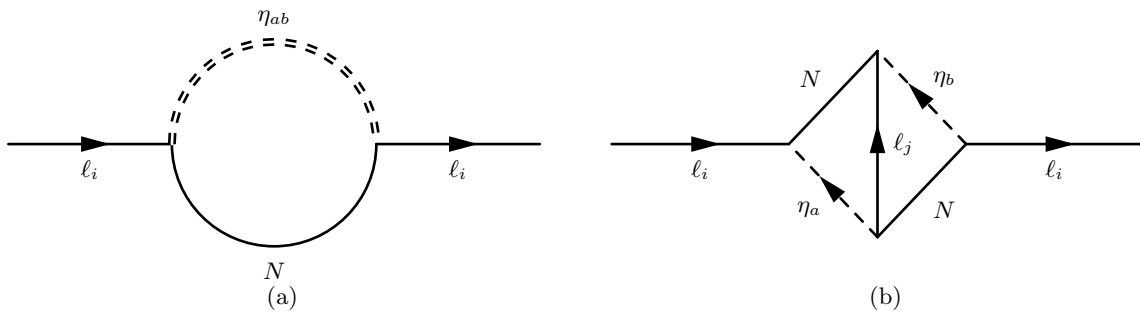


Figure 3: Diagrammatic representation of the CP -violating source terms. The double line for η indicates the summation of the one-loop insertions, which allows for flavor correlations as indicated by the indices ab . Kinematic cuts of these diagrams produce diagrams of the form of Figure 1.

IV. Leptogenesis

In general, Leptogenesis can be described by a set of coupled fluid equations for the particles under consideration, which are then used to track their evolution over time. To account for the expansion of the universe, it is convenient to write the kinetic equations in terms of yields $Y = gn/s$, where g are the internal degrees of freedom of the field, n is the particle number density for a single degree of freedom and s is the entropy density. Since both particle and entropy densities are diluted with the expansion of the universe at the same rate (assuming no entropy is produced), this effect cancels out, and we do not need to include the Hubble rate in the kinetic equations explicitly. We further describe the evolution in terms of the following comoving dimensionful quantities: momentum $\vec{k} = a(t)\vec{k}_{\text{phys}}$, temperature $T = a(t)T_{\text{phys}}$ and entropy $s = a(t)s_{\text{phys}}$, where $a(t)$ is the scale factor from the Friedmann-Lemaître-Robertson-Walker metric. We label the corresponding physical quantities with the subscript phys . We work in conformal time η , which is related to the comoving time t as $dt = ad\eta$, where, in a radiation-dominated universe, $a = a_R\eta$. For the comoving temperature and entropy density we set

$$a_R = T = \frac{m_{Pl}}{2} \sqrt{\frac{45}{g_*\pi^3}}, \quad s = g_* a_R^3 \frac{2\pi^2}{45}, \quad (14)$$

where $m_{Pl} = 1.22 \times 10^{19}$ GeV is the Planck mass and $g_* = 114.75$ is the number of relativistic degrees of freedom with two additional Higgs doublets at high energies so that $\eta = 1/T_{\text{phys}}$. With this setup, the effect of the Hubble expansion on the scattering rates is captured by replacing all masses m by $a(\eta)m$ in the rates that appear in the fluid equations.

For Leptogenesis, this set of equations is given by

$$\frac{dY_N}{dz} = \mathcal{C}_N(Y_N - Y_N^{\text{eq}}), \quad (15)$$

$$\frac{dY_{\ell i}}{dz} = S_{\ell i}(Y_N - Y_N^{\text{eq}}) + W_{\ell i}Y_{\ell i}, \quad (16)$$

with $Y_{\ell i} = g_w q_{\ell i}/s$, $Y_N = g_s n_N/s$, where $q_{\ell i}$ is the charge density of the leptons, n_N is the number density of the Majorana fermion, and g_s, g_w are the spin and $SU(2)$ degrees of freedom respectively. We use $z = M_N/T_{\text{phys}} = M_N\eta$ as a dimensionless time variable.

The CP -violating source term contains a wavefunction and a vertex-type contribution, $S_{\ell i} = S_{\ell i}^{\text{wf}} + S_{\ell i}^{\text{v}}$. In the closed-time-path (CTP) formalism, the wavefunction contribution to the CP -violating source is given by [2]

$$S_{\ell i}^{\text{wf}} = \sum_{a \neq b} Y_i^{(a)*} Y_i^{(b)} \int \frac{d^4 k}{(2\pi)^4} \frac{d^4 p}{(2\pi)^4} \frac{d^4 q}{(2\pi)^4} (2\pi)^4 \delta^4(k + p - q) \text{tr}[iS_N^>(q) iS_{\ell i}^<(k) - \langle \leftrightarrow \rangle] iD_{\eta ab}(p). \quad (17)$$

The corresponding diagram is shown in Figure 3(a). The mixing scalar propagator that follows from the summation of all one-loop insertions is denoted by D_η . Its off-diagonal components can be obtained from the kinetic equation [2, 86, 87]

$$2k^0 \partial_\eta iD_{\eta 12} + i(m_{\eta 1}^2 - m_{\eta 2}^2) iD_{\eta 12} = -\frac{1}{2} i(\Pi_{\eta 12}^{Y>} + \Pi_{\eta 12}^{\lambda>} + \Pi_{\eta 12}^{g>}) i(\Delta_{\eta 11}^< + \Delta_{\eta 22}^<) - \frac{1}{2} \sum_k i(\Pi_{\eta k k}^{Y>} + \Pi_{\eta k k}^{\lambda>} + \Pi_{\eta k k}^{g>}) iD_{\eta 12} - \langle \leftrightarrow \rangle, \quad (18)$$

where the Δ_η are the diagonal scalar propagators, which are assumed to be in thermal equilibrium, and $\Pi_\eta^Y, \Pi_\eta^\lambda, \Pi_\eta^g$ are the scalar self-energies arising from Yukawa, scalar and gauge interactions, respectively. The gauge and scalar interactions effectively bring the mixed propagator into kinetic equilibrium so that we can assume that the solutions to Eq. (18) are of the form [2, 88]

$$iD_{\eta 12}(p) = 2\pi\delta(p^2 - m_{\eta 1}^2) \frac{\mu_{\eta 12}}{T} \frac{\text{sign}(p^0) e^{|p^0|/T}}{(e^{|p^0|/T} - 1)^2}, \quad (19)$$

with the chemical potential $\mu_{\eta 12}$. In principle, the mixed propagator should contain a second contribution with a pole in $m_{\eta 2}$ [86], however, since we assume $m_{\eta 2} \gg m_{\eta 1}$ we can neglect this contribution. In Appendix A we justify the use of the kinetic equilibrium distribution in the propagator. Briefly stated, gauge, scalar, and flavor-conserving Yukawa interactions drive the scalar propagators into equilibrium, while flavor-changing Yukawa interactions with out-of-equilibrium N drive it out of equilibrium. We can then parametrize the correlations between the two mass eigenstates of η with a chemical potential $\mu_{\eta 12}$, which is proportional to μ_N , the chemical potential for N .

Following Ref. [3], we can integrate Eq. (18) over the momentum k where we separate the integrals for positive and negative k^0 . Defining

$$n_{12}^\pm = 2 \int_0^{\pm\infty} \frac{dk^0}{2\pi} \int \frac{d^3k}{(2\pi)^3} k^0 iD_{\eta 12}(k), \quad (20)$$

we then obtain

$$\pm i(m_{\eta 1}^2 - m_{\eta 2}^2)n_{12}^\pm = -B_\eta^Y - B_\eta^{Y,\#} n_{12}^\pm - B_\eta^g(n_{12}^+ + n_{12}^-) - B_\eta^{\lambda,\text{even}} n_{12}^\pm - B_\eta^{\lambda,\text{odd}} n_{12}^\mp, \quad (21)$$

with the solution

$$q_{\eta 12} = n_{12}^+ - n_{12}^- = \mathcal{R}_\eta 2iB_\eta^Y, \quad (22a)$$

$$\mathcal{R}_\eta = \frac{m_{\eta 1}^2 - m_{\eta 2}^2}{(m_{\eta 1}^2 - m_{\eta 2}^2)^2 + (B_\eta^{Y,\#} + B_\eta^{\lambda,\text{even}} - B_\eta^{\lambda,\text{odd}})(B_\eta^{Y,\#} + 2B_\eta^g + B_\eta^{\lambda,\text{even}} + B_\eta^{\lambda,\text{odd}})}. \quad (22b)$$

Here, B_η^Y and $B_\eta^{Y,\#}$ are averaged rates for Yukawa-mediated flavor sensitive and flavor blind reactions, respectively, $B_\eta^{\lambda,\text{even}}$ and $B_\eta^{\lambda,\text{odd}}$ are the rates for scalar-mediated charge even and odd interactions, while B_η^g is the averaged rate of (flavor blind) gauge processes. They are estimated in Appendix B. We can then relate the charge $q_{\eta 12}$ to the chemical potential $\mu_{\eta 12}$ with

$$q_{\eta 12} = 2 \int \frac{d^4k}{(2\pi)^4} k^0 iD_{\eta 12}(k) = \frac{\mu_{\eta 12} T^2}{3}. \quad (23)$$

As for the vertex contribution to the CP -violating term, the source term is given by

$$S_{\ell i}^V = \int \frac{d^4k}{2\pi} \text{tr}[i\Sigma_\ell^{V,>}(k) iS_\ell^{<}(k) - i\Sigma_\ell^{V,<}(k) iS_\ell^{>}(k)], \quad (24)$$

with [89]

$$\begin{aligned} i\Sigma_i^{V,ab}(k) = & -cdY_i^{(a)*} Y_j^{(a)} Y_j^{(b)*} Y_i^{(b)} \int \frac{d^4p}{(2\pi)^4} \frac{d^4q}{(2\pi)^4} P_R iS_N^{ac}(-p) C[P_L iS_{\ell j}^{dc}(p+k+q) P_R]^t C^\dagger \\ & \times iS_N^{db}(-q) P_L i\Delta_{\eta a}^{da}(-p-k) i\Delta_{\eta b}^{bc}(-q-k). \end{aligned} \quad (25)$$

We present a detailed derivation of the vertex contribution in Appendix C.

The equilibration rates for N and ℓ at tree-level are given by [2, 3]

$$c_N = - \sum_i \left| Y_i^{(1)} \right|^2 \frac{a_R}{8\pi M_N} z \frac{K_1(z)}{K_2(z)} \approx - \sum_i \left| Y_i^{(1)} \right|^2 \frac{a_R}{8\pi M_N} z \equiv c_N z, \quad (26)$$

$$W_{\ell i} = - \left| Y_i^{(1)} \right|^2 \frac{3a_R}{8\pi^3 M_N} z^3 K_1(z) \approx - \left| Y_i^{(1)} \right|^2 3 \times 2^{-7/2} \pi^{-5/2} \frac{a_R}{M_N} z^{5/2} e^{-z} \equiv c_{W_i} z^{5/2} e^{-z}, \quad (27)$$

while for the source terms we find

$$\begin{aligned} S_{\ell i}^{\text{wf}} = & \mathcal{R}_\eta \text{Im}[Y_i^{(1)} Y_j^{(1)*} Y_j^{(2)} Y_i^{(2)*}] \frac{3a_R M_N z^5}{2^6 \pi^4} K_1(z) \\ & \approx \mathcal{R}_\eta \text{Im}[Y_i^{(1)} Y_j^{(1)*} Y_j^{(2)} Y_i^{(2)*}] 3 \times 2^{-13/2} \pi^{-7/2} a_R M_N z^{5/2} e^{-z} \equiv c_{S_i}^{\text{wf}} z^{5/2} e^{-z}. \end{aligned} \quad (28)$$

and

$$\begin{aligned}
S_{\ell i}^v &= \text{Im}[Y_i^{(1)} Y_j^{(1)*} Y_j^{(2)} Y_i^{(2)*}] \frac{M_N^2}{m_2^2} \frac{a_R}{M_N} \frac{1}{2^8 \pi^2} \frac{(6\sqrt{6}K_1(\sqrt{6}z)/z + 4K_0(\sqrt{6}z))}{K_2(z)} \\
&\approx \text{Im}[Y_i^{(1)} Y_j^{(1)*} Y_j^{(2)} Y_i^{(2)*}] \frac{M_N^2}{m_2^2} \frac{a_R}{M_N} \pi^{-2} 2^{-25/4} 3^{-1/4} e^{(1-\sqrt{6})z} \equiv c_{S_i^v}^v e^{(1-\sqrt{6})z}.
\end{aligned} \tag{29}$$

Note that, since $m_{\eta 2} \gg M_N, m_{\eta 1}$, the Yukawa couplings to η_2 do not enter the equilibration rates Eqs. (26) and (27). In addition, we have

$$Y_N^{\text{eq}} \approx \frac{2}{s} \int \frac{d^3 k}{(2\pi)^3} e^{-k^0/T} = \pi^{-2} a_R^3 z^2 K_2(z)/s \approx 2^{-1/2} \pi^{-3/2} a_R^3 z^{3/2} e^{-z}/s \equiv c_Y z^{3/2} e^{-z}. \tag{30}$$

Since Eq. (16) is linear in $Y_{\ell i}$, we can decompose it into two equations

$$\frac{dY_{\ell i}^{\text{wf},v}}{dz} = S_{\ell i}^{\text{wf},v}(Y_N - Y_N^{\text{eq}}) + W_{\ell i} Y_{\ell i}^{\text{wf},v}, \tag{31}$$

and add the two solutions to obtain the total yield. We can formally integrate the kinetic equations and obtain, for vanishing initial lepton asymmetry

$$Y_{\ell i}(z) = \int_{z_i}^z S_{\ell i}(z') (Y_N - Y_N^{\text{eq}})(z') e^{\int_{z'}^z W_{\ell i}(z'') dz''} dz' = \int_{z_i}^z \frac{S_{\ell i}(z')}{C_N(z')} \frac{dY_N}{dz'} e^{\int_{z'}^z W_{\ell i}(z'') dz''} dz', \tag{32}$$

which, in the strong washout regime, we can approximate as

$$Y_{\ell i}(z) = \int_{z_i}^z \frac{S_{\ell i}(z')}{C_N(z')} \frac{dY_N^{\text{eq}}}{dz'} e^{\int_{z'}^z W_{\ell i}(z'') dz''} dz'. \tag{33}$$

Using Laplace's method, we can express the final asymmetries as [90]

$$Y_{\ell i}^{\text{wf}}(z = \infty) = -\frac{c_{S_i}^{\text{wf}}}{c_N} c_Y \left(z_{\text{fi},\text{wf}} - \frac{3}{2} \right) z_{\text{fi},\text{wf}}^2 \sqrt{\frac{2\pi e^{z_{\text{fi},\text{wf}}}}{c_{W_i}(5/2 z_{\text{fi},\text{wf}}^{3/2} - z_{\text{fi},\text{wf}}^{5/2})}} e^{-\int_{z_{\text{fi},\text{wf}}}^{\infty} c_{W_i} z'^{5/2} e^{-z'} dz' - 2z_{\text{fi},\text{wf}}}, \tag{34}$$

and

$$Y_{\ell i}^v(z = \infty) = -\frac{c_{S_i}^v}{c_N} c_Y \left(z_{\text{fi},v} - \frac{3}{2} \right) z_{\text{fi},v}^{-1/2} \sqrt{\frac{2\pi e^{z_{\text{fi},v}}}{c_{W_i}(5/2 z_{\text{fi},v}^{3/2} - z_{\text{fi},v}^{5/2})}} e^{-\int_{z_{\text{fi},v}}^{\infty} c_{W_i} z'^{5/2} e^{-z'} dz' - \sqrt{6} z_{\text{fi},v}}, \tag{35}$$

with

$$z_{\text{fi},\text{wf}} = -\frac{5}{2} W_{-1} \left(-\frac{2}{5} \times \left(\frac{2}{c_{W_i}} \right)^{2/5} \right), \tag{36}$$

and

$$z_{\text{fi},v} = -\frac{5}{2} W_{-1} \left(-\frac{2}{5} \times \frac{6^{1/5}}{c_{W_i}^{2/5}} \right), \tag{37}$$

where W_{-1} is the lower branch of the Lambert W function.

The lepton asymmetry obtained is then transferred to the baryon sector through sphalerons. We can relate the final yield to the baryon asymmetry of the Universe through [91, 92]

$$\eta_B = \frac{n_B}{n_\gamma} = 7.04 \times Y_{\ell i} \frac{24 + 4N_\phi}{66 + 13N_\phi}, \tag{38}$$

where N_ϕ is the number of Higgs doublets, in our case $N_\phi = 3$, and compare with the value obtained by the Planck collaboration [93]

$$\eta_B = (6.143 \pm 0.190) \times 10^{-10}. \tag{39}$$

V. Dark Matter Production

Given the mass relations we choose for this model, η_1 , being the lightest particle in the Z_2 -odd sector, is absolutely stable and therefore a natural dark matter candidate. This situation is similar to inert doublet models (IDM), which have been studied extensively in the literature [85, 94]. Being a scalar doublet, there is a wide range of processes that contribute to its annihilation rate, both via electroweak interactions and through the additional scalar couplings. We derive the Feynman rules for the model using FeynRules [95] and compute the DM properties using micrOMEGAs [96]. We choose $\lambda_5 < 0$ and set $\lambda_3 = \lambda_4 = -0.4\lambda_5$ as benchmark values. We then perform a scan of the DM relic abundance and cross-section varying m_{η_1} and compare with the Planck measurement $\Omega h_{\text{DM}}^2 = 0.120 \pm 0.001$ [93] and with LUX-ZEPLIN constraints [83], respectively, as shown in Figure 4. For the comparison with LUX-ZEPLIN data, we rescale the cross section as $\hat{\sigma} = \sigma \Omega_{\text{DM}} / \Omega_{\text{DM}}^{\text{Planck}}$, i.e. we assume the local dark matter density to coincide with the value of the cosmological average.

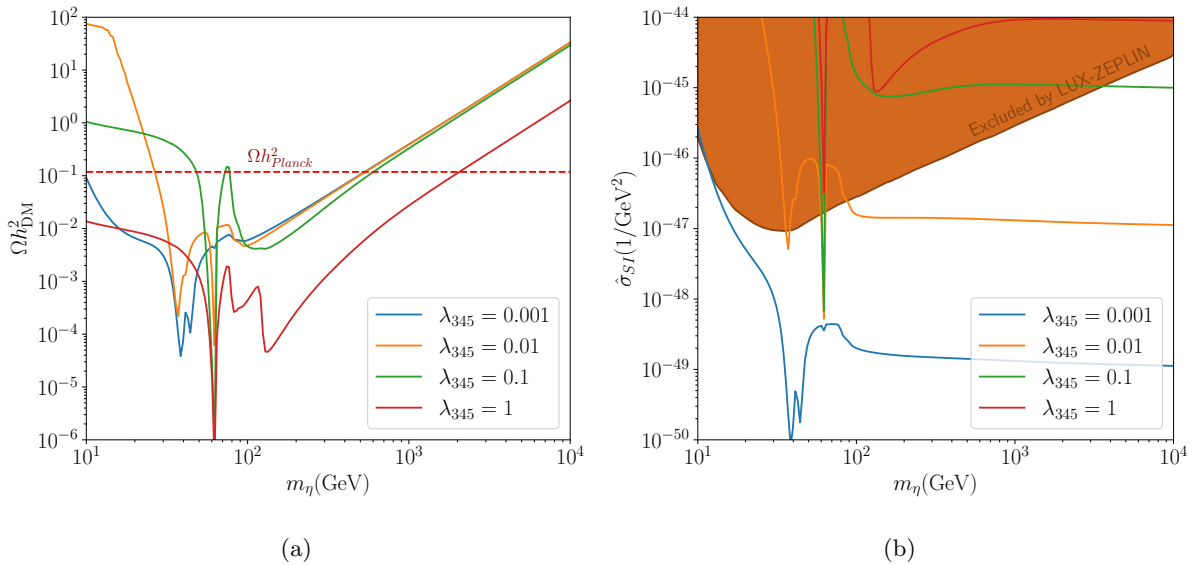


Figure 4: Scan of dark matter relic abundance (a) and spin-independent cross-section (b) in m_{η} for different values of λ compared with the Planck measurement [93] and with LUX-ZEPLIN constraints [83], respectively.

To avoid the overproduction of dark matter, a large m_{η} needs to be compensated by large scalar couplings, which are constrained by direct detection. However, the direct detection bounds can be evaded if there are cancellations between λ_3, λ_4 and λ_5 in λ_{345} ; in this case, the strongest constraint comes from the requirement of perturbativity. Combining both constraints, we find that m_{η} must lie between around 375 GeV and 1000 GeV to be able to produce the correct relic abundance.

VI. Finding the Joint Parameter Space

The present model has the following free parameters: the Yukawa matrix Y , the masses $M_N, m_{\eta_1}, m_{\eta_2}$, and the scalar couplings λ . Since the Yukawa matrix, and therefore the neutrino mass matrix, has rank two, we can reduce the neutrino mass matrix to a 2×2 matrix, which, in the neutrino mass eigenbasis, is given by

$$m_{\nu} = Y \Lambda Y^T = \begin{pmatrix} m_2 & 0 \\ 0 & m_3 \end{pmatrix}, \quad (40)$$

where we define

$$\Lambda^{(ab)} = \frac{\lambda_5^{(ab)} v^2}{8\pi^2} \frac{M_N}{m_{\eta_b}^2 - M_N^2} \left(\frac{m_{\eta_b}^2}{m_{\eta_a}^2 - m_{\eta_b}^2} \log \left(\frac{m_{\eta_a}^2}{m_{\eta_b}^2} \right) - \frac{M_N^2}{m_{\eta_a}^2 - M_N^2} \log \left(\frac{m_{\eta_a}^2}{M_N^2} \right) \right). \quad (41)$$

For fixed Yukawa matrix Y and particle masses, we can invert relation Eq. (40) to obtain

$$\lambda_5^{(ab)} = \left(Y^{-1} \begin{pmatrix} m_2 & 0 \\ 0 & m_3 \end{pmatrix} (Y^T)^{-1} \right)^{(ab)} / \tilde{\Lambda}^{(ab)}, \quad (42)$$

with $\tilde{\Lambda}^{(ab)} = \Lambda^{(ab)} / \lambda_5^{(ab)}$.

The lepton asymmetry is produced in two lepton flavors with opposite signs. We therefore need different washout rates $c_{W1} \neq c_{W2}$, otherwise the asymmetries would exactly cancel, and the final asymmetry is maximized in the strongly hierarchical case $c_{Wi} \gg c_{Wj}$. In addition to this, the mass splitting between the two neutral components is proportional to $\text{Re}(\lambda_5^{(11)})$ per Eq. (12), which we also want to maximize, in order to avoid the direct detection via Z -boson exchange. We further choose $\text{Re}(\lambda_5^{(11)}) < 0$. We find that setting $\phi(Y_1^{(1)}) = \pi/4$, $\phi(Y_2^{(1)}) = -\pi/4$ and $\phi(Y_1^{(2)}) = \phi(Y_2^{(2)})$ arbitrary, we maximize the CP -violating phase and obtain $\phi(\lambda_5^{(11)}) = \pi$.

For scanning the parameter space, we fix $|Y_2^{(1)}| = 0.1|Y_1^{(1)}|$ and $m_{\eta_1} = 750 \text{ GeV}$. Furthermore, since the impact of the Yukawa couplings to η_2 on the equilibration and washout rates are negligible, they are arbitrary. For illustrative purposes, we set $|Y_1^{(2)}| = |Y_2^{(2)}| = 10^3|Y_1^{(1)}|$. Increasing this ratio can lead to Leptogenesis scales down to 10^7 GeV , but even ratios down to 10 give an allowed parameter region. The parameter scan with the relevant constraints is shown in Fig. 5.

We find there is a region, albeit small, of values consistent with all bounds. Except for the baryon asymmetry, all bounds follow similar curves, which essentially depend on λ_5 . From Equations (6), (41) and (42), we see that decreasing $|Y_1|$ and increasing M_N leads to an increase in λ_5 . Small values of λ_5 are constrained first because this would lead to DM overproduction (red region) and a small mass splitting between m_R and m_I , making it susceptible to direct detection via neutral currents, while large values of λ_5 would violate perturbativity and would be inconsistent with direct detection bounds.

VII. Experimental Signatures

As discussed in Section III, the main experimental constraints come from lepton flavor violation and direct detection experiments. Due to the very large mass of N , lepton flavor violating processes are strongly suppressed, and an improvement of many orders of magnitude in LFV precision measurements is required before a signal from our model is expected. On the other hand, we find that LUX-ZEPLIN places stringent bounds on the scalar couplings of the new doublets. While, as we have argued in Section V, detection can be avoided in case of cancellations between λ_3, λ_4 and λ_5 , large cancellations would require severe fine-tuning.

A third detection prospect is via missing transverse energy in collider experiments. For these searches, our model has essentially the same signatures as the inert Higgs doublet model, whose main detection channels for collider searches include: mono-jet production ($pp \rightarrow \eta_R \eta_R j$), mono- Z production ($pp \rightarrow \eta_R \eta_R Z$), mono-Higgs production ($gg \rightarrow \eta_R \eta_R H$ and $q\bar{q} \rightarrow \eta_R \eta_R H$) and vector boson fusion ($pp \rightarrow \eta \eta jj$) for hadron colliders as well as $e^+e^- \rightarrow \eta_R \eta_I$ and $e^+e^- \rightarrow \eta^+ \eta^-$ for electron-positron colliders [94, 97–106]. It was found that masses up to $\gtrsim 300 \text{ GeV}$ can be probed at the HL-LHC [101, 103, 104], which, while unable to explain all of the dark matter within our model, is also a viable scenario. This can be improved with higher center-of-mass energies, for instance in ILC or CLIC, which can potentially probe masses up to 1 TeV [105, 106].

VIII. Conclusion

In this work we have investigated the simultaneous neutrino mass generation, DM production, and Leptogenesis from a minimal realization of the Scotogenic model, with two additional scalar doublets and a single Majorana fermion only, odd under a \mathbb{Z}_2 symmetry.

The Leptogenesis mechanism we consider is via heavy Majorana fermion decay, where the decay asymmetry arises from the mixing and interferences between the two dark scalars. In our treatment of Leptogenesis we have included an improved estimate of the scalar propagator width which strongly limits the resonant enhancement of the asymmetry. Due to the large width of the propagator, we find that in some regions of the parameter space vertex contributions to the CP -violating source term can become more relevant than the resonant wavefunction contributions. We also find that, on the one hand, large quartic couplings for the new scalars are needed to avoid the overproduction of dark matter, while on the other hand, direct detection experiments place stringent bounds on these quartic couplings, which can only be evaded if some cancellation between the scalar couplings occurs.

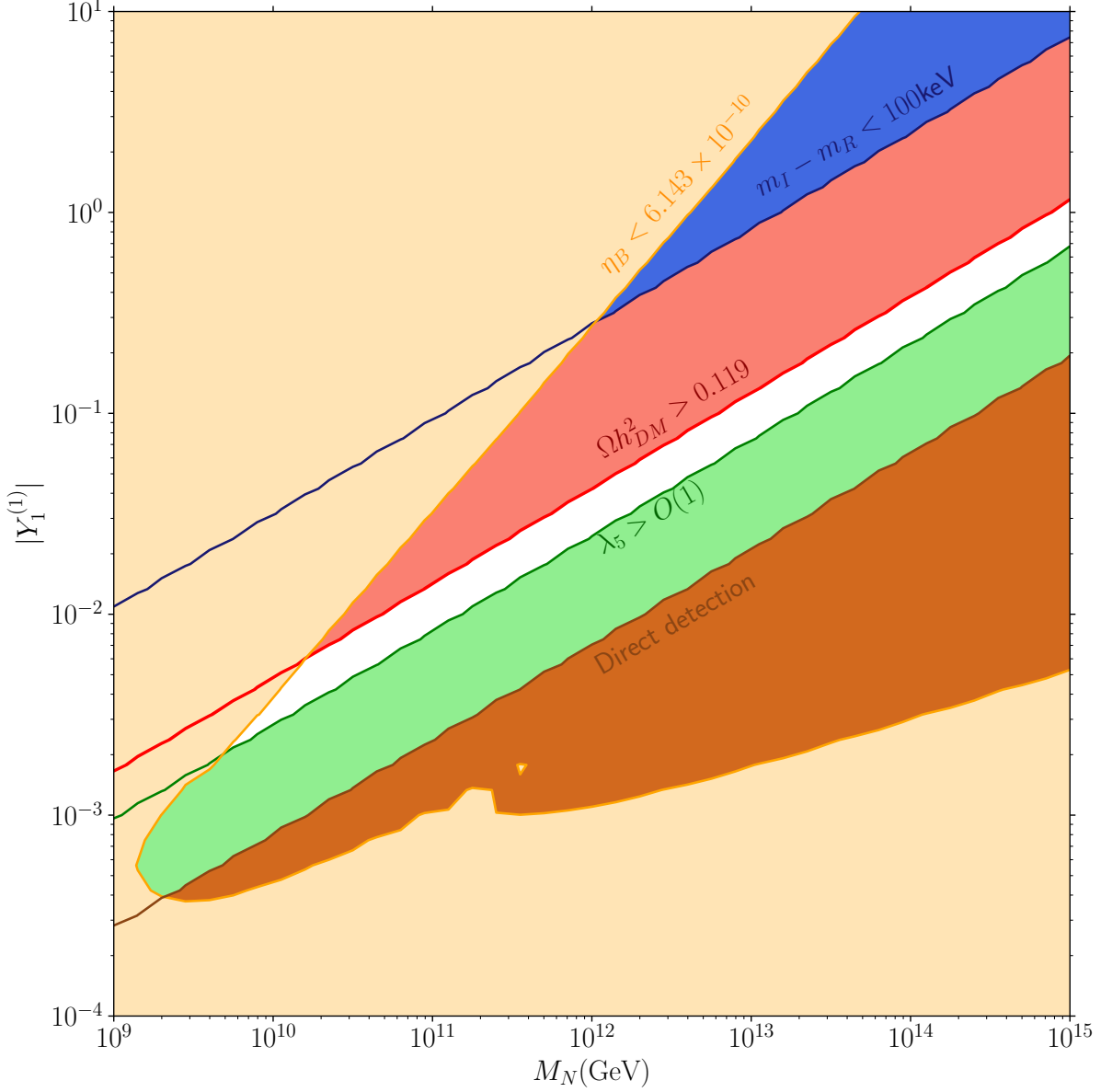


Figure 5: Allowed region (white) for M_N and $|Y_1^{(1)}|$ in the hierarchy $m_{\eta_2} > M_N > m_{\eta_1}$. We fix the ratios $|Y_2^{(1)}| = 0.1|Y_1^{(1)}|$ as well as $|Y_1^{(2)}| = |Y_2^{(2)}| = 10^3|Y_1^{(1)}|$ and $m_{\eta_2} = 10M_N$, and set $m_{\eta_1} = 750$ GeV. The orange region cannot account for the BAU, the blue line is where the mass splitting of the neutral scalars is too small to prevent upscattering via Z -boson exchange. The red line marks the constraint from dark matter overproduction, and the green line is where scalar interactions become larger than $O(1)$. The brown line is the direct detection bound from LUX-ZEPLIN.

Nevertheless, performing a scan of M_N and of the Yukawa couplings, for $500 \text{ GeV} < m_\eta < 1000 \text{ GeV}$ we find a region of parameter space consistent with all constraints, which could explain the neutrino masses, account for the dark matter and the baryon asymmetry of the Universe simultaneously. Since there is a single Majorana fermion in the model, the CP -violating processes differ substantially from those in standard Leptogenesis. In particular, these involve the interference of new particles that, while in the dark sector, are not Standard Model singlets. In the future, it may be interesting to pursue similar possibilities more broadly.

Acknowledgements

EW's work is supported by the Collaborative Research Center SFB 1258 of the German Research Foundation. We would also like to thank Carlos Tamarit for useful discussions.

A. Kinetic Equilibration of the Propagator

In order for Eq. (19) to hold, kinetic equilibrium has to be established for the scalar doublets η . Since N is out of equilibrium, Π^Y drives iD_{12} also out of equilibrium. Since we do not make assumptions about the distribution of N , it is not immediately clear why iD_{12} can still be taken to be of the form of a kinetic equilibrium distribution. This approximation, which is often used for calculations in different scenarios for baryogenesis, shall be justified in the present appendix. From the kinetic equations for the resummed scalar propagator we have [86, 87]

$$2k^0 \partial_t iD_{ij}^{<, >} + i(m_{\eta i}^2 - m_{\eta j}^2) iD_{ij}^{<, >} = -\frac{1}{2} (i\Pi_{ik}^{>} iD_{kj}^{<} + i\Pi_{kj}^{>} iD_{ik}^{<} - i\Pi_{ik}^{<} iD_{kj}^{>} - i\Pi_{kj}^{<} iD_{ik}^{>}). \quad (\text{A1})$$

In the current discussion, we only include contributions to the self-energy from Yukawa and gauge interactions, Π^Y and Π^g respectively. For the moment, consider the case where $\Pi^Y = (M_1^2 - m_{\eta 2}^2) = 0$, so that the scalar particles are degenerate in their masses and interactions and that there are only gauge interactions. Looking for stationary solutions, Eq. (A1) then reduces to

$$i\Pi_{ik}^{>} iD_{kj}^{<} + i\Pi_{kj}^{>} iD_{ik}^{<} - i\Pi_{ik}^{<} iD_{kj}^{>} - i\Pi_{kj}^{<} iD_{ik}^{>} = 0. \quad (\text{A2})$$

This can be solved by assuming that the propagators follow a kinetic equilibrium distribution, writing, as in Ref. [88],

$$iD_{ab}^{<}(k) = 2\pi\delta(k^2)[\theta(k^0)f_{ab}^\mu(k) + \theta(-k^0)(\mathbb{1}_{ab} + \bar{f}_{ab}^\mu(k))], \quad (\text{A3a})$$

$$iD_{ab}^{>}(k) = 2\pi\delta(k^2)[\theta(k^0)(\mathbb{1}_{ab} + f_{ab}^\mu(k)) + \theta(-k^0)\bar{f}_{ab}^\mu(k)], \quad (\text{A3b})$$

with

$$f_{ab}^\mu(k) = \left(\frac{1}{e^{(|k|-\mu)/T} - 1} \right)_{ab}, \quad \bar{f}_{ab}^\mu(k) = \left(\frac{1}{e^{(|k|+\mu)/T} - 1} \right)_{ab}, \quad (\text{A4})$$

where we have introduced a matrix of chemical potentials μ_{ab} . With this we obtain a generalized Kubo-Martin-Schwinger (KMS) relation for the propagators in kinetic equilibrium

$$D_{ab}^{>}(k) = (e^{(k^0-\mu)/T})_{ac} D_{cb}^{<}(k) = D_{ac}^{<}(k) (e^{(k^0-\mu)/T})_{cb}. \quad (\text{A5})$$

To see that Eqs. (A3) hold, note that the self-energy contribution from gauge interactions is given by

$$i\Pi_{ab}^{g,cd}(k) = g^2 \int \frac{d^4 k'}{(2\pi)^4} \frac{d^4 k''}{(2\pi)^4} (2\pi)^4 \delta^4(k - k' - k'') iD_{ab}^{cd}(k') k''^\mu k''^\nu i\Delta_{\mu\nu}^{cd}(k''), \quad (\text{A6})$$

where a, b are CTP indices, c, d are flavor indices and $i\Delta_{\mu\nu}$ is the full gauge boson propagator. Since $i\Delta$ is in thermal equilibrium, it also observes the KMS relation. We then find that

$$i\Pi_{ab}^{g,>}(k) = (e^{(k^0-\mu)/T})_{ac} \Pi_{cb}^{g,<}(k) = \Pi_{ac}^{g,<}(k) (e^{(k^0-\mu)/T})_{cb}, \quad (\text{A7})$$

where the last equality follows from the fact that $(e^{(k^0-\mu)/T})$ and D commute. With this we find

$$i\Pi_{ik}^{>} iD_{kj}^{<} = i\Pi_{il}^{<} (e^{(k^0-\mu)/T})_{lk} (e^{-(k^0-\mu)/T})_{km} iD_{mj}^{>} = i\Pi_{ik}^{<} iD_{kj}^{>}, \quad (\text{A8})$$

and verify that Eq. (A2) is indeed satisfied. To first order in the chemical potentials, we can approximate

$$f_{ab}^\mu(k) = \mathbb{1}_{ab} \frac{1}{e^{|k|/T} - 1} + \frac{\mu_{ab}}{T} \frac{e^{|k|/T}}{(e^{|k|/T} - 1)^2}. \quad (\text{A9})$$

We now restrict the discussion to the components of the propagator accounting for mixing of the scalar flavors, i.e. $iD_{12}^{<} = iD_{12}^{>} = iD_{12}$. The kinetic equation for this part of the propagator is

$$i(m_{\eta 1}^2 - m_{\eta 2}^2) iD_{12} = -\frac{1}{2} ((i\Pi_{12}^{Y,>} + i\Pi_{12}^{g,>})(iD_{11}^{<} + iD_{22}^{<}) + (i\Pi_{11}^{Y,>} + i\Pi_{11}^{g,>} + i\Pi_{22}^{Y,>} + i\Pi_{22}^{g,>}) iD_{12- <\leftrightarrow>}). \quad (\text{A10})$$

with the stationary solution

$$iD_{12} = \frac{1}{-i(m_{\eta_1}^2 - m_{\eta_2}^2) + i\Pi^A} \left(-\frac{1}{2}(i\Pi_{12}^{Y,>} + i\Pi_{12}^{g,>})(iD_{11}^< + iD_{22}^<) - \langle\leftrightarrow\rangle \right). \quad (\text{A11})$$

While Π^g contains iD , Π^Y does not, since to leading order it only entails a fermion loop. Defining

$$A^{g,cd}(k, k') = g^2 \int \frac{d^4 k''}{(2\pi)^4} (2\pi)^4 \delta^4(k - k' - k'') k''^\mu k''^\nu i\Delta_{\mu\nu}^{cd}(k''), \quad (\text{A12})$$

we can rewrite the kinetic equation as

$$\begin{aligned} i(m_{\eta_1}^2 - m_{\eta_2}^2)iD_{12}(k) &= -\frac{1}{2}(i\Pi_{12}^{Y,>}(k)(iD_{11}^<(k) + iD_{22}^<(k)) + (i\Pi_{11}^{Y,>}(k) + i\Pi_{22}^{Y,>}(k))iD_{12}(k) \\ &\quad + \int \frac{d^4 k'}{(2\pi)^4} iA^{g,>}(k, k')[(iD_{11}^>(k') + iD_{22}^>(k'))iD_{12}(k) \\ &\quad + iD_{12}(k')(iD_{11}^<(k) + iD_{22}^<(k))] - \langle\leftrightarrow\rangle). \end{aligned} \quad (\text{A13})$$

We now define $f(-k^0) = \bar{f}(|k^0|)$ and insert the form of the propagators given in Eqs. (A3). We then find that Eq. (A13) takes the form

$$i(m_{\eta_1}^2 - m_{\eta_2}^2)f_{12}(k^0) = A_{\text{const}}^Y(k^0) + A_{\text{diag}}^Y(k^0)f_{12}(k^0) + A_{\text{diag}}^g(k^0)f_{12}(k^0) + \int \frac{dk'^0}{2\pi} A_{\text{non-diag}}^g(k, k'^0)f_{12}(k'^0), \quad (\text{A14})$$

where we have introduced the short-hand notation

$$A_{\text{const}}^Y(k^0) = -\frac{1}{2}i\Pi_{12}^{Y,>}(k)(f_{11}(k^0) + f_{22}(k^0)), \quad (\text{A15a})$$

$$A_{\text{diag}}^Y(k^0) = -\frac{1}{2}(i\Pi_{11}^{Y,>}(k) + i\Pi_{22}^{Y,>}(k)), \quad (\text{A15b})$$

$$A_{\text{diag}}^g(k^0) = \int \frac{dk'^4}{(2\pi)^4} iA^{g,>}(k, k')[(iD_{11}^>(k') + iD_{22}^>(k')) - \langle\leftrightarrow\rangle], \quad (\text{A15c})$$

$$A_{\text{non-diag}}^g(k, k'^0) = \int \frac{dk'^3}{(2\pi)^3} 2\pi\delta(k'^2) iA^{g,>}(k, k')[(f_{11}(k^0) + f_{22}(k^0)) - \langle\leftrightarrow\rangle]. \quad (\text{A15d})$$

The subscripts here indicate the dependence on f_{12} , i.e. whether the terms on the right-hand side of Eq. (A14) are independent of f_{12} and if they are dependent, whether they are diagonal or generally nondiagonal in k^0 .

When we discretize the momentum k^0 , we obtain

$$i(m_{\eta_1}^2 - m_{\eta_2}^2)f_{12}(k_i) = A_{\text{const}}^Y(k_i) + (A_{\text{diag}}^Y(k_i) + A_{\text{diag}}^g(k_i))f_{12}(k_i) + \sum_j \frac{\Delta k}{2\pi} A_{\text{non-diag}}^g(k_i, k_j)f_{12}(k_j), \quad (\text{A16})$$

which we can interpret as a matrix equation

$$R_{ij}f_{12}(k_j) = yv_i, \quad (\text{A17})$$

where y is a new expansion parameter which we tag to all quantities driving the distribution out of equilibrium.

a. Quasi-degenerate case Here, the mass splitting $m_{\eta_1}^2 - m_{\eta_2}^2$ as well as the interactions mediated by Y are small compared to the gauge interactions mediated by g . The latter thus have time to establish kinetic equilibrium also in the off-diagonal correlations. We thus decompose R as

$$v_i = A_{\text{const}}^Y(k_i), \quad (\text{A18})$$

$$R_{ij} = R_{ij}^g + yR_{ij}^Y = -A_{\text{diag}}^g(k_i)\delta_{ij} - \frac{\Delta k}{2\pi} A_{\text{non-diag}}^g(k_i, k_j) - y(A_{\text{diag}}^Y(k_i) - i(m_{\eta_1}^2 - m_{\eta_2}^2))\delta_{ij}, \quad (\text{A19})$$

Clearly, the solution to Eq. (A17) is

$$f_{12}(k_i) = yR_{ij}^{-1}v_j. \quad (\text{A20})$$

We also recover the pure gauge scenario when we send $y \rightarrow 0$, in which case Eq. (A17) becomes

$$R_{ij}^g f_{12}(k_j) = 0, \quad (\text{A21})$$

whose solution is precisely the chemical equilibrium distribution f_{12}^μ , as we have seen before. From this equation we also recognize that R_{ij}^g is singular. Then, following Ref. [107], we can regard R_{ij} as a matrix function in y and expand $R_{ij}^{-1}(y)$ as a Laurent series in y

$$M^{-1}(y) = \frac{1}{y^s} (X_0 + yX_1 + \dots), \quad (\text{A22})$$

where s is the order of the pole at $y = 0$. We expect the kernel of T^g to be one-dimensional, and if it is not simultaneously the kernel of R^Y , using the method introduced in Ref. [108], we find that R^{-1} has a simple pole at the origin, and from the condition

$$RR^{-1} = \mathbb{1}, \quad (\text{A23})$$

we obtain the fundamental equations

$$R^g X_0 = 0, \quad (\text{A24a})$$

$$R^g X_1 + R^Y X_0 = \mathbb{1}, \quad (\text{A24b})$$

$$R^g X_2 + R^Y X_1 = 0, \quad (\text{A24c})$$

⋮

With these equations, we can find $X_0, X_1 \dots$ and write our problem as

$$f_{12}(k) = X_0 v^Y + y X_1 v^Y + \mathcal{O}(y^2). \quad (\text{A25})$$

To zeroth order in y , the solution Eq. (A20) is given by $X_0 v^Y$, but from Eq. (A24a), we know that $M^g X_0 v^Y = 0$, which means that $X_0 v^Y$ lies in the kernel of M^g . Since the kernel of M^g is one-dimensional, this implies that $X_0 v^Y$ is proportional to $f_{12}^\mu(k)$, and therefore, if the gauge interactions are much stronger than the Yukawa interactions and the squared mass difference of the η , f_{12} can indeed be approximated by f_{12}^μ , the kinetic equilibrium distribution.

b. Non-degenerate case So far we have treated the mass splitting as a perturbation compared to the gauge self-energies. We now want to treat the case where the mass splitting dominates the kinetic equation. The gauge interactions then do not have time to impose kinetic equilibrium on the off-diagonal correlations induced by the out-of-equilibrium Majorana fermion. In this case, we can rewrite Eq. (A17) as

$$(i\Delta M_\eta^2 \mathbb{1} - M^{g+Y})_{ij} f_{12}(k_j) = v_i, \quad (\text{A26})$$

where

$$v_i = A_{\text{const}}^Y(k_i), \quad (\text{A27})$$

$$R_{ij}^{g+Y} = A_{\text{diag}}^g(k_i) \delta_{ij} + \frac{\Delta k}{2\pi} A_{\text{non-diag}}^g(k_i, k_j) + A_{\text{diag}}^Y(k_i) \delta_{ij}. \quad (\text{A28})$$

We can divide Eq. (A26) by $i\Delta M_\eta^2$ and obtain

$$\left(\mathbb{1} - \frac{M^{g+Y}}{i\Delta M_\eta^2} \right)_{ij} f_{12}(k_j) = \frac{v_i}{i\Delta M_\eta^2}, \quad (\text{A29})$$

with the solution

$$f_{12}(k_i) = \left(\mathbb{1} - \frac{M^{g+Y}}{i\Delta M_\eta^2} \right)_{ij}^{-1} \frac{v_j}{i\Delta M_\eta^2}. \quad (\text{A30})$$

Since we assume $|i\Delta M_\eta^2| \gg |M^{g+Y}|$, we can write $(\mathbb{1} - M^{g+Y}/(i\Delta M_\eta^2))^{-1}$ as a Neumann series

$$\left(\mathbb{1} - \frac{M^{g+Y}}{i\Delta M_\eta^2} \right)^{-1} = \sum_k \left(\frac{M^{g+Y}}{i\Delta M_\eta^2} \right)^k. \quad (\text{A31})$$

Since higher order terms are suppressed by powers of $1/\Delta M_\eta^2$, we can keep only the leading order term, which gives us

$$f_{12}(k_i) = \frac{v_i}{i\Delta M_\eta^2}. \quad (\text{A32})$$

Going back to Eq. (A11), this means we can approximate

$$iD_{12} \approx \frac{1}{-i(m_{\eta_1}^2 - m_{\eta_2}^2)} \left(-\frac{1}{2} i\Pi_{12}^{Y,>} (iD_{11}^< + iD_{22}^<) - \langle \leftrightarrow \rangle \right). \quad (\text{A33})$$

If we parametrize the deviation of N from equilibrium with a pseudo-chemical potential μ_N , we find again a KMS relation for Π_{12}^Y :

$$i\Pi_{12}^{Y,>}(k) = e^{(k^0 - \mu_N)/T} i\Pi_{12}^{Y,<}(k), \quad (\text{A34})$$

from which we can rewrite Eq. (A33) as

$$iD_{12}(k) = \frac{1}{-i(m_{\eta_1}^2 - m_{\eta_2}^2)} 2\Pi_{12}^{Y,\mathcal{A}}(k) \Delta_{\eta_1}^{\mathcal{A}}(k) \frac{\text{sign}(k^0)(1 - e^{-\mu_N/T})e^{k^0/T}}{(e^{(k^0 - \mu_N)/T} - 1)(e^{k^0/T} - 1)}, \quad (\text{A35})$$

where we have omitted the contribution from Δ_{η_2} since we assume η_2 to be much heavier than η_1 , and can therefore neglect its on-shell contribution. To first order in the chemical potential we can write

$$iD_{12}(k) = 2\pi\delta(k^2 - m_{\eta_1}^2) \frac{1}{-i(m_{\eta_1}^2 - m_{\eta_2}^2)} \Pi_{12}^{Y,\mathcal{A}}(k) \frac{\mu_N}{T} \frac{\text{sign}(k^0)e^{|k^0|/T}}{(e^{|k^0|/T} - 1)^2}. \quad (\text{A36})$$

In the regime of interest, $m_{\eta_1} \gg T$, the dominant contributions arise for $\mathbf{k} \ll T$ and $|k^0| - m_{\eta_1} \ll T$, so that we can neglect the k dependence of $\Pi_{12}^{Y,\mathcal{A}}(k)$ and rewrite this as

$$iD_{12}(k) = 2\pi\delta(k^2 - m_{\eta_1}^2) \frac{\mu_{\eta_{12}}}{T} \frac{\text{sign}(k^0)e^{|k^0|/T}}{(e^{|k^0|/T} - 1)^2}, \quad (\text{A37})$$

where we have introduced a new chemical potential $\mu_{\eta_{12}}$, chosen in such a way that both definitions produce the same charges. So we can again apply Eq. (19). Note that while the approximation does not apply in the exponential tail, it holds for the relevant momentum range.

With this we have shown that we can parametrize f_{12} with a chemical potential both in the case where the kinetic equation (A1) is dominated by gauge (or other) interactions driving it to kinetic equilibrium as well as when it is dominated by the mass splitting.

B. Spectral Self-Energies

To determine the width of the mixed scalar propagator from the kinetic equation (18), we need to compute the spectral self-energies for the fields. The two main contributions come from the Yukawa and the gauge interactions. In Eq. (21) we have introduced the averaged rates, which are defined as

$$B_{\eta}^Y = \pm \int_0^{\pm\infty} \frac{dk^0}{2\pi} \int \frac{d^3k}{(2\pi)^3} k^0 i\Pi_{12}^{Y,>}(k) (i\Delta_{\eta_{11}}^<(k) + i\Delta_{\eta_{22}}^<(k)) - \langle \leftrightarrow \rangle, \quad (\text{B1})$$

$$B_{\eta}^{Y,\mathcal{A}} = \pm \frac{1}{n_{12}^{\pm}} \int_0^{\pm\infty} \frac{dk^0}{2\pi} \int \frac{d^3k}{(2\pi)^3} 2k^0 (\Pi_{11}^{Y,\mathcal{A}}(k) + \Pi_{22}^{Y,\mathcal{A}}(k)) iD_{\eta_{12}}(k), \quad (\text{B2})$$

$$B_{\eta}^g = \pm \frac{1}{n_{12}^{\pm}} \int_0^{\pm\infty} \frac{dk^0}{2\pi} \int \frac{d^3k}{(2\pi)^3} 2k^0 (\Pi_{11}^{g,\mathcal{A}}(k) + \Pi_{22}^{g,\mathcal{A}}(k)) iD_{\eta_{12}}(k), \quad (\text{B3})$$

$$B_{\eta}^{\lambda,\text{even}} n_{12}^{\pm} + B_{\eta}^{\lambda,\text{odd}} n_{12}^{\mp} = \pm \int_0^{\pm\infty} \frac{dk^0}{2\pi} \int \frac{d^3k}{(2\pi)^3} k^0 \sum_k (i\Pi_{12}^> i\Delta_{\eta_{kk}}^< + i\Pi_{kk}^> iD_{\eta_{12}} - \langle \leftrightarrow \rangle). \quad (\text{B4})$$

Using CTP methods and assuming $M_N \gg T$, we find [3]

$$B_{\eta}^Y = [Y^{\dagger}Y]_{12} \frac{M_N^4 \mu_N}{32\pi^3} K_2(M_N/T), \quad (\text{B5})$$

where μ_N is a chemical potential we introduce to parametrize the deviation of N from equilibrium. The Yukawa spectral self-energy can be computed at first order, giving

$$\Pi_{ab}^{Y,\mathcal{A}}(k) = -\text{sign}(k^0) \frac{[Y^{\dagger}Y]_{ab}}{16\pi k^0} T M_N^2 e^{-M_N^2/(4|k^0|T)}, \quad (\text{B6})$$

where we have approximated the distribution of the Majorana neutrinos N as nonrelativistic. We then find

$$B_\eta^{Y,\#} = \sum_j (Y_j^{(1),2} + Y_j^{(2),2}) \frac{3}{32\pi^3} \frac{M_N^4}{T^2} K_2(M_N/T). \quad (\text{B7})$$

Defining the reduced cross section for a two-body scattering as

$$\hat{\sigma}(s) = \frac{2\lambda(s, m_1, m_2)}{s} \sigma(s), \quad (\text{B8})$$

where σ is the usual cross-section and λ is the function

$$\lambda(s, m_1, m_2) = \sqrt{(s - (m_1 + m_2)^2)(s - (m_1 - m_2)^2)}, \quad (\text{B9})$$

one can compute the reaction density as

$$\gamma = \frac{T}{64\pi^4} \int_{(m_1+m_2)^2}^{\infty} ds \hat{\sigma}(s) \sqrt{s} K_1\left(\frac{\sqrt{s}}{T}\right). \quad (\text{B10})$$

We present here a detailed derivation of B^λ , which, to the best of our knowledge, is computed for the first time. The relevant contribution to the self-energy comes from the sunset diagram and is given by

$$i\Pi^{\lambda ab}(k) = \sum \lambda^\dagger \lambda \int \frac{d^4 p}{(2\pi)^4} \frac{d^4 p'}{(2\pi)^4} i\Delta_\phi^{ab}(p) i\Delta_{\phi/\eta}^{ab}(p') i\Delta_{\eta/\phi}^{ba}(p + p' - k), \quad (\text{B11})$$

where $\lambda^\dagger \lambda$ stands for the coupling structure and the sum is over the field configurations running in the loop. We also choose a signature where all temporal momenta have the same sign (since the expression is symmetric under exchange of the momenta, this can always be done). The collision term is then

$$\begin{aligned} \mathcal{C} &= \sum_k (i\Pi_{12}^> i\Delta_{kk}^< + i\Pi_{kk}^> iD_{12} - i\Pi_{12}^< i\Delta_{kk}^> - i\Pi_{kk}^< iD_{12}) \\ &= \sum_{k,j \neq \ell} \int \frac{d^4 p}{(2\pi)^4} \frac{d^4 p'}{(2\pi)^4} \frac{d^4 k'}{(2\pi)^4} (2\pi)^4 \delta^4(k + k' - p - p') \\ &\times \left\{ i\Delta_\phi^>(p) \left[\lambda_5^{1j} \lambda_5^{\ell 2*} i\Delta_\phi^>(p') iD_{\eta j \ell}(k') + (\lambda_3^{1j} + \lambda_4^{j1} + \text{h.c.}) (\lambda_3^{\ell 2*} + \lambda_4^{2\ell*} + \text{h.c.}) iD_{\eta j \ell}(p') i\Delta_\phi^<(k') \right] i\Delta_{\eta k k}^<(k) \right. \\ &+ i\Delta_\phi^>(p) \left[\lambda_5^{k\ell} \lambda_5^{\ell k*} i\Delta_\phi^>(p') i\Delta_{\eta \ell \ell}^<(k') + (\lambda_3^{k\ell} + \lambda_4^{\ell k} + \text{h.c.}) (\lambda_3^{\ell k*} + \lambda_4^{k\ell*} + \text{h.c.}) i\Delta_{\eta \ell \ell}^>(p') i\Delta_\phi^<(k') \right] iD_{\eta 12}(k) \\ &- i\Delta_\phi^<(p) \left[\lambda_5^{1j} \lambda_5^{\ell 2*} i\Delta_\phi^<(p') iD_{\eta j \ell}(k') + (\lambda_3^{1j} + \lambda_4^{j1} + \text{h.c.}) (\lambda_3^{\ell 2*} + \lambda_4^{2\ell*} + \text{h.c.}) iD_{\eta j \ell}(p') i\Delta_\phi^>(k') \right] i\Delta_{\eta k k}^>(k) \\ &\left. - i\Delta_\phi^<(p) \left[\lambda_5^{k\ell} \lambda_5^{\ell k*} i\Delta_\phi^<(p') i\Delta_{\eta \ell \ell}^>(k') + (\lambda_3^{k\ell} + \lambda_4^{\ell k} + \text{h.c.}) (\lambda_3^{\ell k*} + \lambda_4^{k\ell*} + \text{h.c.}) i\Delta_{\eta \ell \ell}^<(p') i\Delta_\phi^>(k') \right] iD_{\eta 12}(k) \right\}. \quad (\text{B12}) \end{aligned}$$

While $D_{\eta 12}$ also contributes wherever $\Delta_{\eta \ell \ell}$ appears, this would be a higher order correction, which we discard as we only consider linear terms in the off-diagonal correlations of the particles $\eta_{1,2}$. Similarly, $\Delta_{\eta \ell \ell}$ also should contribute where $D_{\eta j \ell}$ appears, but since we assume diagonal propagators to be in equilibrium, this would give a purely equilibrium, and therefore vanishing, contribution. Since $m_{\eta 2} \gg T$, we can also neglect $\Delta_{\eta 22}$ contributions, since they are strongly Maxwell-suppressed. Lastly, we see that not only $D_{\eta 12}$ appears in the collision term but also $D_{\eta 21}$, implying that there is some mixing between n_{12} and n_{21} . We also neglect this term to avoid complicating the problem even further. The full reaction rate is obtained by integrating the collision term over k , and, in spite of the complicated flavor structure, we can approximate all processes as having the same $2 \leftrightarrow 2$ kinematics. Paying particular attention to the signs of the contributions, this gives us

$$\begin{aligned} \Gamma^{\lambda, \pm} &= \int_0^{\pm\infty} \frac{dk^0}{2\pi} \int \frac{d^3 k}{(2\pi)^3} \mathcal{C}(k) \\ &= \frac{\Gamma}{2} [(\lambda_5^{11} \lambda_5^{22*} - (\lambda_3^{11} + \lambda_4^{11} + \text{h.c.}) (\lambda_3^{22*} + \lambda_4^{22*} + \text{h.c.})) (n_{12}^\pm - 2n_{12}^\mp) \\ &\quad + 3 \sum_k (\lambda_5^{k1} \lambda_5^{1k*} + (\lambda_3^{k1} + \lambda_4^{1k} + \text{h.c.}) (\lambda_3^{1k*} + \lambda_4^{k1*} + \text{h.c.})) n_{12}^\pm], \\ &\equiv \Gamma^{\lambda, \text{even}} n_{12}^\pm + \Gamma^{\lambda, \text{odd}} n_{12}^\mp, \quad (\text{B13}) \end{aligned}$$

where we divide by two to average over the $SU(2)$ degrees of freedom, and

$$\Gamma = \frac{1}{n^{\text{eq}}} \int \frac{d^3k}{(2\pi)^{3/2}|k^0|} \frac{d^3k'}{(2\pi)^{3/2}|k'^0|} \frac{d^3p}{(2\pi)^{3/2}|p^0|} \frac{d^3p'}{(2\pi)^{3/2}|p'^0|} (2\pi)^4 \delta^4(k+k'-p-p') f(k) f(k') \quad (\text{B14})$$

$$= \frac{T}{16\pi^2},$$

in Boltzmann approximation. Then, with the approximation that all particles have the same reaction rate regardless of momentum, we can write [3]

$$Bn_{12}^{\pm} = \int \frac{d^3k}{(2\pi)^3} |k| \Gamma f_{12}(k) = n_{12}^{\pm} \frac{36}{\pi^2} \Gamma T. \quad (\text{B15})$$

As for gauge interactions, since we are in a regime where the gauge bosons are massless, the first-order self-energy corresponding to $1 \leftrightarrow 2$ processes vanishes. We therefore need to go to second order, which corresponds to two-by-two scatterings. The only relevant scatterings are pair creation and annihilation since they are the only ones that can change particle number. We use FeynArts [109] to generate the relevant diagrams and FeynCalc [110–112] to obtain the corresponding amplitudes. As opposed to earlier estimates from Ref. [3], IR divergences in t and u -channel cancel, and these contributions can be directly accounted for. The total reduced cross-section we find is

$$\hat{\sigma}(s) = \frac{1}{12} (327g_1^4 + 42g_1^2g_2^2 + 169g_2^4), \quad (\text{B16})$$

from which we obtain the reaction density

$$\gamma^g = \frac{T}{64\pi^4} \int_0^\infty ds \sqrt{s} K_1 \left(\frac{\sqrt{s}}{T} \right) \hat{\sigma}(s) = \frac{T^4}{192\pi^4} (327g_1^4 + 42g_1^2g_2^2 + 169g_2^4). \quad (\text{B17})$$

From this, following Ref. [3], using $g_2 = 0.6$ and $g_1 = 0.4$ we find

$$B_\eta^g = \frac{36}{\pi^2} \Gamma^g T = \frac{36}{\pi^2} \frac{\gamma^g}{3/(2\pi)^2 \zeta(3) T^2} = 1.4 \times 10^{-3} T^2, \quad (\text{B18})$$

which is one order of magnitude larger than the expression in Ref. [3].

C. Vertex Contribution to the Source Term

The vertex contribution to the CP -source is given by

$$\begin{aligned} S_{\ell i}^v &= \int \frac{d^4k}{(2\pi)^4} \text{tr}[i\Sigma_\ell^>(k) iS_\ell^<(k) - i\Sigma_\ell^<(k) iS_\ell^>(k)] \\ &= \int \frac{d^4k}{(2\pi)^4} \frac{d^4p}{(2\pi)^4} \frac{d^4q}{(2\pi)^4} \text{tr}[-Y_i^{(a)*} Y_j^{(a)} Y_j^{(b)*} Y_i^{(b)} \{i\delta S_N(-p) C[iS_{\ell j}^T(p+k+q) i\Delta_{\eta b}^T(-q-k) \\ &\quad - iS_{\ell j}^<(p+k+q) i\Delta_{\eta b}^<(-q-k)]^t C^\dagger iS_N^T(-q) i\Delta_{\eta a}^<(-p-k) \\ &\quad + iS_N^T(-p) C[iS_{\ell j}^T(p+k+q) i\Delta_{\eta a}^T(-p-k) - iS_{\ell j}^<(p+k+q) i\Delta_{\eta a}^<(-p-k)]^t C^\dagger i\Delta_{\eta b}^<(-q-k) \\ &\quad i\delta S_N(-q)\} iS_{\ell i}^<(k)] - (+ \leftrightarrow -). \end{aligned} \quad (\text{C1})$$

Dropping on-shell η_2 terms, we have

$$\begin{aligned} S_{\ell i}^v &= \int \frac{dk_0}{2\pi} \frac{d^4p}{(2\pi)^4} \frac{d^4q}{(2\pi)^4} \\ &\text{tr}[\{-Y_i^{(1)*} Y_j^{(1)} Y_j^{(2)*} Y_i^{(2)} i\delta S_N(-p) C[iS_{\ell j}^T(p+k+q)]^t C^\dagger i\Delta_{\eta_2}^T(-q-k) iS_N^T(-q) i\Delta_{\eta_1}^<(-p-k) \\ &\quad + Y_i^{(1)} Y_j^{(1)*} Y_j^{(2)} Y_i^{(2)*} iS_N^T(-p) C[iS_{\ell j}^T(p+k+q)]^t C^\dagger i\Delta_{\eta_2}^T(-p-k) i\Delta_{\eta_1}^<(-q-k) i\delta S_N(-q)\} iS_{\ell i}^<(k) \\ &\quad + \{-Y_i^{(1)*} Y_j^{(1)} Y_j^{(2)*} Y_i^{(2)} i\delta S_N(-p) C[iS_{\ell j}^T(p+k+q)]^t C^\dagger i\Delta_{\eta_2}^T(-q-k) iS_N^T(-q) i\Delta_{\eta_1}^>(-p-k) \\ &\quad + Y_i^{(1)} Y_j^{(1)*} Y_j^{(2)} Y_i^{(2)*} iS_N^T(-p) C[iS_{\ell j}^T(p+k+q)]^t C^\dagger i\Delta_{\eta_2}^T(-p-k) i\Delta_{\eta_1}^>(-q-k) i\delta S_N(-q)\} iS_{\ell i}^>(k)], \end{aligned} \quad (\text{C2})$$

where we have used $i\Delta_{\eta_2}^T = -i\Delta_{\eta_2}^{\bar{T}}$ for off-shell η_2 .

As was argued in Ref. [89], we only need to keep the absorptive parts of $iS_{\ell}^{T,\bar{T}}$ and $iS_N^{T,\bar{T}}$, since the dispersive parts cancel upon integration. We then have

$$S_{\ell i}^v = -4\text{Im}[Y_i^{(1)}Y_j^{(1)*}Y_j^{(2)}Y_i^{(2)*}] \int \frac{d^3p}{(2\pi)^3 2p^0} \frac{d^3k}{(2\pi)^3 2k^0} \frac{d^3p'}{(2\pi)^3 2p'^0} \frac{d^3q}{(2\pi)^3 2q^0} \frac{d^3q'}{(2\pi)^3 2q'^0} \delta^4(q - q' - p') \delta^4(p - k - q')$$

$$(k \cdot p') \delta f_N(p) f_{\ell j}(p') f_N(q) \frac{M_N^2}{(q+k)^2 - m_{\eta_2}^2} (1 + f_{\eta_1}(q') - f_{\ell i}(k)).$$

We can use the spatial delta functions to carry out the p' and the k integrals. Neglecting quantum statistical factors, we then have

$$S_{\ell i}^v = -4\text{Im}[Y_i^{(1)}Y_j^{(1)*}Y_j^{(2)}Y_i^{(2)*}] \int \frac{d^3p}{(2\pi)^3 2p^0} \frac{d^3q}{(2\pi)^3 2q^0} \frac{d^3q'}{(2\pi)^3 2q'^0} \frac{1}{2k^0} \frac{1}{2p'^0} (2\pi)^2 \delta(q^0 - q'^0 - p'^0) \delta(p^0 - k^0 - q'^0)$$

$$((q - q') \cdot (p - q')) \delta f_N(p) f_{\ell j}(q - q') f_N(q) \frac{M_N^2}{(q+k)^2 - m_{\eta_2}^2}.$$

We can use spherical coordinates to express p and q with respect to q' through the angles $\theta_{p,q}, \varphi_{p,q}$ and use the delta functions to do the $\theta_{p,q}$ integrals. Approximating $M_N^2/((q+k)^2 - m_{\eta_2}^2) \approx -M_N^2/m_{\eta_2}^2$, we have

$$S_{\ell i}^v = 4\text{Im}[Y_i^{(1)}Y_j^{(1)*}Y_j^{(2)}Y_i^{(2)*}] \int \frac{d^3q'}{(2\pi)^3 2q'^0} \int_{|q'-M_N^2/(4q')|}^{\infty} \frac{dp}{2\pi} \frac{d\varphi_p p^2}{(2\pi) 2p^0} \int_{|q'-M_N^2/(4q')|}^{\infty} \frac{dq}{2\pi} \frac{d\varphi_q q^2}{(2\pi) 2q^0}$$

$$\frac{1}{2pq'} \frac{1}{2qq'} (2M_N^2(q - q') \cdot (p - q')) \delta f_N(p) f_{\ell j}(q - q') f_N(q) \frac{M_N^2}{m_{\eta_2}^2}.$$

We express

$$(q - q') \cdot (p - q') = -\frac{1}{4}pq \sqrt{-\frac{M_N^2(4q'(q' - p^0) + M_N^2)}{p^2 q'^2}} \sqrt{-\frac{M_N^2(4q'(q' - q^0) + M_N^2)}{q^2 q'^2}} \cos(\varphi_p - \varphi_q)$$

$$-\frac{(M_N^2 - 4q'^2)(M_N^2 - 2q'(p^0 + q^0))}{4q'^2}.$$

The first term vanishes when performing the φ integrals, and we are left with

$$S_{\ell i}^v = 4\text{Im}[Y_i^{(1)}Y_j^{(1)*}Y_j^{(2)}Y_i^{(2)*}] \frac{M_N^2}{m_{\eta_2}^2} \int \frac{d^3q'}{(2\pi)^3 2q'^0} \int_{|q'-M_N^2/(4q')|}^{\infty} \frac{dp}{2\pi} \frac{p}{2p^0} \int_{|q'-M_N^2/(4q')|}^{\infty} \frac{dq}{2\pi} \frac{q}{2q^0}$$

$$\times \frac{1}{2q'} \frac{1}{2q'} \frac{(M_N^2 - 4q'^2)(M_N^2 - 2q'(p^0 + q^0))}{4q'^2} \delta f_N(p) f_{\ell j}(q - q') f_N(q)$$

$$= 4\text{Im}[Y_i^{(1)}Y_j^{(1)*}Y_j^{(2)}Y_i^{(2)*}] \frac{M_N^2}{m_{\eta_2}^2} \frac{T^2}{32\pi^3}$$

$$\times \int \frac{dq' q'}{2\pi} \frac{(M_N^2 - 4q'^2)(2M_N^2 - 8q' \sqrt{(q' - M_N^2/(4q'))^2 + M_N^2} - 6q'T)}{64q'^4} e^{-3\sqrt{(q' - M_N^2/(4q'))^2 + M_N^2}/T} e^{q'/T}.$$

Since we assume $M_N \gg T$, we can approximate

$$\sqrt{(q' - M_N^2/(4q'))^2 + M_N^2} \approx \frac{M_N^2}{4q} + q. \quad (\text{C3})$$

With this we can evaluate the above integral and obtain

$$S_{\ell i}^v = 4\text{Im}[Y_i^{(1)}Y_j^{(1)*}Y_j^{(2)}Y_i^{(2)*}] \frac{M_N^2}{m_{\eta_2}^2} \frac{T^2}{64\pi^4} \frac{1}{32} (6\sqrt{6}M_N T K_1(\sqrt{6}M_N/T) + 4M_N^2 K_0(\sqrt{6}M_N/T)). \quad (\text{C4})$$

Dividing by

$$n_N = \frac{1}{2\pi^2} M_N^2 T K_2(M_N/T), \quad (\text{C5})$$

and shifting to comoving coordinates, we find

$$S_{\ell i}^v = \text{Im}[Y_i^{(1)}Y_j^{(1)*}Y_j^{(2)}Y_i^{(2)*}] \frac{M_N^2}{m_2^2} \frac{a_R}{M_N} \frac{1}{2^8 \pi^2} \frac{(6\sqrt{6}K_1(\sqrt{6}z)/z + 4K_0(\sqrt{6}z))}{K_2(z)}. \quad (\text{C6})$$

-
- [1] M. Fukugita and T. Yanagida, Baryogenesis Without Grand Unification, *Phys. Lett. B* **174**, 45 (1986).
- [2] B. Garbrecht, Leptogenesis from Additional Higgs Doublets, *Phys. Rev. D* **85**, 123509 (2012), arXiv:1201.5126 [hep-ph].
- [3] B. Garbrecht, Baryogenesis from Mixing of Lepton Doublets, *Nucl. Phys. B* **868**, 557 (2013), arXiv:1210.0553 [hep-ph].
- [4] C. Hagedorn, J. Herrero-García, E. Molinaro, and M. A. Schmidt, Phenomenology of the Generalised Scotogenic Model with Fermionic Dark Matter, *JHEP* **11**, 103, arXiv:1804.04117 [hep-ph].
- [5] N. Kumar, T. Nomura, and H. Okada, Scotogenic neutrino mass with large $SU(2)_L$ multiplet fields, *Eur. Phys. J. C* **80**, 801 (2020), arXiv:1912.03990 [hep-ph].
- [6] P. Escribano, M. Reig, and A. Vicente, Generalizing the Scotogenic model, *JHEP* **07**, 097, arXiv:2004.05172 [hep-ph].
- [7] J. Leite, A. Morales, J. W. F. Valle, and C. A. Vaquera-Araujo, Dark matter stability from Dirac neutrinos in scotogenic 3-3-1-1 theory, *Phys. Rev. D* **102**, 015022 (2020), arXiv:2005.03600 [hep-ph].
- [8] M. Sarazin, J. Bernigaud, and B. Herrmann, Dark matter and lepton flavour phenomenology in a singlet-doublet scotogenic model, *JHEP* **12**, 116, arXiv:2107.04613 [hep-ph].
- [9] A. Ahriche, A scotogenic model with two inert doublets, *JHEP* **02**, 028, arXiv:2208.00500 [hep-ph].
- [10] A. Alvarez, A. Banik, R. Cepedello, B. Herrmann, W. Porod, M. Sarazin, and M. Schnelke, Accommodating muon ($g - 2$) and leptogenesis in a scotogenic model, *JHEP* **06**, 163, arXiv:2301.08485 [hep-ph].
- [11] C. Bonilla, A. E. Carcamo Hernandez, J. Goncalves, V. K. N., A. P. Morais, and R. Pasechnik, Gravitational waves from a scotogenic two-loop neutrino mass model, (2023), arXiv:2305.01964 [hep-ph].
- [12] P. Escribano, V. M. Lozano, and A. Vicente, Scotogenic explanation for the 95 GeV excesses, *Phys. Rev. D* **108**, 115001 (2023), arXiv:2306.03735 [hep-ph].
- [13] A. Karan, S. Sadhukhan, and J. W. F. Valle, Phenomenological profile of scotogenic fermionic dark matter, *JHEP* **12**, 185, arXiv:2308.09135 [hep-ph].
- [14] M. Maniatis, A. von Manteuffel, O. Nachtmann, and F. Nagel, Stability and symmetry breaking in the general two-Higgs-doublet model, *Eur. Phys. J. C* **48**, 805 (2006), arXiv:hep-ph/0605184.
- [15] V. Keus, S. F. King, and S. Moretti, Three-Higgs-doublet models: symmetries, potentials and Higgs boson masses, *JHEP* **01**, 052, arXiv:1310.8253 [hep-ph].
- [16] X.-Q. Li, J. Lu, and A. Pich, $B_{s,d}^0 \rightarrow \ell^+ \ell^-$ Decays in the Aligned Two-Higgs-Doublet Model, *JHEP* **06**, 022, arXiv:1404.5865 [hep-ph].
- [17] M. Maniatis and O. Nachtmann, Stability and symmetry breaking in the general three-Higgs-doublet model, *JHEP* **02**, 058, [Erratum: *JHEP* 10, 149 (2015)], arXiv:1408.6833 [hep-ph].
- [18] C.-H. Chen and T. Nomura, Two-Higgs-Doublet Type-II Seesaw Model, *Phys. Rev. D* **90**, 075008 (2014), arXiv:1406.6814 [hep-ph].
- [19] G. Abbas, A. Celis, X.-Q. Li, J. Lu, and A. Pich, Flavour-changing top decays in the aligned two-Higgs-doublet model, *JHEP* **06**, 005, arXiv:1503.06423 [hep-ph].
- [20] M. Maniatis, D. Mehta, and C. M. Reyes, Stability and symmetry breaking in a three-Higgs-doublet model with lepton family symmetry $O(2) \otimes \mathbb{Z}_2$, *Phys. Rev. D* **92**, 035017 (2015), arXiv:1503.05948 [hep-ph].
- [21] T. Han, S. K. Kang, and J. Sayre, Muon $g - 2$ in the aligned two Higgs doublet model, *JHEP* **02**, 097, arXiv:1511.05162 [hep-ph].
- [22] Q.-Y. Hu, X.-Q. Li, and Y.-D. Yang, $B^0 \rightarrow K^{*0} \mu^+ \mu^-$ decay in the Aligned Two-Higgs-Doublet Model, *Eur. Phys. J. C* **77**, 190 (2017), arXiv:1612.08867 [hep-ph].
- [23] Q.-Y. Hu, X.-Q. Li, and Y.-D. Yang, The $\Lambda_b \rightarrow \Lambda(\rightarrow p\pi^-) \mu^+ \mu^-$ decay in the aligned two-Higgs-doublet model, *Eur. Phys. J. C* **77**, 228 (2017), arXiv:1701.04029 [hep-ph].
- [24] G. Abbas, D. Das, and M. Patra, Loop induced $H^\pm \rightarrow W^\pm Z$ decays in the aligned two-Higgs-doublet model, *Phys. Rev. D* **98**, 115013 (2018), arXiv:1806.11035 [hep-ph].
- [25] D. Cogollo, R. D. Matheus, T. B. de Melo, and F. S. Queiroz, Type I + II Seesaw in a Two Higgs Doublet Model, *Phys. Lett. B* **797**, 134813 (2019), arXiv:1904.07883 [hep-ph].
- [26] D. Jurčiukonis, T. Gajdosik, and A. Juodagalvis, Seesaw neutrinos with one right-handed singlet field and a second Higgs doublet, *JHEP* **11**, 146, arXiv:1909.00752 [hep-ph].
- [27] C.-H. Chen, C.-W. Chiang, and T. Nomura, Muon $g-2$ in a two-Higgs-doublet model with a type-II seesaw mechanism, *Phys. Rev. D* **104**, 055011 (2021), arXiv:2104.03275 [hep-ph].
- [28] S.-W. Wang, Study of $B_s \rightarrow D_s^* \tau \bar{\nu}$ Decay in the Aligned Two-Higgs-Doublet Model and Vector Leptoquark Model, *Int. J. Theor. Phys.* **60**, 3225 (2021).
- [29] K. Enomoto, S. Kanemura, and Y. Mura, New benchmark scenarios of electroweak baryogenesis in aligned two Higgs double models, *JHEP* **09**, 121, arXiv:2207.00060 [hep-ph].
- [30] L. Sartore, M. Maniatis, I. Schienbein, and B. Herrmann, The general Two-Higgs Doublet Model in a gauge-invariant form, *JHEP* **12**, 051, arXiv:2208.13719 [hep-ph].
- [31] F.-M. Cai, S. Funatsu, X.-Q. Li, and Y.-D. Yang, Rare top-quark decays $t \rightarrow cg(g)$ in the aligned two-Higgs-doublet model, *Eur. Phys. J. C* **82**, 881 (2022), arXiv:2202.08091 [hep-ph].
- [32] J. M. Connell, P. Ferreira, and H. E. Haber, Accommodating hints of new heavy scalars in the framework of the flavor-aligned two-Higgs-doublet model, *Phys. Rev. D* **108**, 055031 (2023), arXiv:2302.13697 [hep-ph].
- [33] A. Karan, V. Miralles, and A. Pich, Updated global fit of the aligned two-Higgs-doublet model with heavy scalars, *Phys. Rev. D* **109**, 035012 (2024), arXiv:2307.15419 [hep-ph].

- [34] N. Darvishi, A. Pilaftsis, and J.-H. Yu, Maximising CP Violation in Naturally Aligned Two-Higgs Doublet Models, (2023), arXiv:2312.00882 [hep-ph].
- [35] G. Arcadi and S. Khan, Axion Dark Matter and additional BSM aspects in an extended 2HDM setup, (2023), arXiv:2312.17099 [hep-ph].
- [36] A. C. B. Machado and V. Pleitez, A model with two inert scalar doublets, *Annals Phys.* **364**, 53 (2016), arXiv:1205.0995 [hep-ph].
- [37] E. C. F. S. Fortes, A. C. B. Machado, J. Montaña, and V. Pleitez, Scalar dark matter candidates in a two inert Higgs doublet model, *J. Phys. G* **42**, 105003 (2015), arXiv:1407.4749 [hep-ph].
- [38] V. Keus, S. F. King, S. Moretti, and D. Sokolowska, Dark Matter with Two Inert Doublets plus One Higgs Doublet, *JHEP* **11**, 016, arXiv:1407.7859 [hep-ph].
- [39] V. Keus, S. F. King, and S. Moretti, Phenomenology of the inert (2+1) and (4+2) Higgs doublet models, *Phys. Rev. D* **90**, 075015 (2014), arXiv:1408.0796 [hep-ph].
- [40] T. Alanne, K. Kainulainen, K. Tuominen, and V. Vaskonen, Baryogenesis in the two doublet and inert singlet extension of the Standard Model, *JCAP* **08**, 057, arXiv:1607.03303 [hep-ph].
- [41] A. Aranda, D. Hernández-Otero, J. Hernández-Sánchez, V. Keus, S. Moretti, D. Rojas-Ciofalo, and T. Shindou, Z_3 symmetric inert (2+1)-Higgs-doublet model, *Phys. Rev. D* **103**, 015023 (2021), arXiv:1907.12470 [hep-ph].
- [42] M. Merchand and M. Sher, Constraints on the Parameter Space in an Inert Doublet Model with two Active Doublets, *JHEP* **03**, 108, arXiv:1911.06477 [hep-ph].
- [43] G. Belanger, A. Mjallal, and A. Pukhov, WIMP and FIMP dark matter in the inert doublet plus singlet model, *Phys. Rev. D* **106**, 095019 (2022), arXiv:2205.04101 [hep-ph].
- [44] M. O. Khojali, A. Abdalgabar, A. Ahriche, and A. S. Cornell, Dark matter in a singlet-extended inert Higgs-doublet model, *Phys. Rev. D* **106**, 095039 (2022), arXiv:2206.06211 [hep-ph].
- [45] S. Singirala, D. K. Singha, and R. Mohanta, Neutrino magnetic moment and inert doublet dark matter in a Type-III radiative scenario, *Phys. Rev. D* **108**, 095048 (2023), arXiv:2306.14801 [hep-ph].
- [46] P. W. Angel, Y. Cai, N. L. Rodd, M. A. Schmidt, and R. R. Volkas, Testable two-loop radiative neutrino mass model based on an $LLQd^c Qd^c$ effective operator, *JHEP* **10**, 118, [Erratum: *JHEP* **11**, 092 (2014)], arXiv:1308.0463 [hep-ph].
- [47] A. Addazi, ‘Exotic vector-like pair’ of color-triplet scalars, *JHEP* **04**, 153, arXiv:1501.04660 [hep-ph].
- [48] A. Addazi and M. Bianchi, Un-oriented Quiver Theories for Majorana Neutrons, *JHEP* **07**, 144, arXiv:1502.01531 [hep-ph].
- [49] E. Carquin, N. A. Neill, J. C. Helo, and M. Hirsch, Exotic colored fermions and lepton number violation at the LHC, *Phys. Rev. D* **99**, 115028 (2019), arXiv:1904.07257 [hep-ph].
- [50] G. R. Dvali, Can ‘doublet - triplet splitting’ problem be solved without doublet - triplet splitting?, *Phys. Lett. B* **287**, 101 (1992).
- [51] G. R. Dvali, Light color triplet Higgs is compatible with proton stability: An Alternative approach to the doublet - triplet splitting problem, *Phys. Lett. B* **372**, 113 (1996), arXiv:hep-ph/9511237.
- [52] Y. Kawamura, Triplet doublet splitting, proton stability and extra dimension, *Prog. Theor. Phys.* **105**, 999 (2001), arXiv:hep-ph/0012125.
- [53] G. von Gersdorff, A Clockwork Solution to the Doublet-Triplet Splitting Problem, *Phys. Lett. B* **813**, 136039 (2021), arXiv:2009.08480 [hep-ph].
- [54] A. Pilaftsis, Loop induced CP violation in the gaugino and Higgsino sectors of supersymmetric theories, *Phys. Rev. D* **62**, 016007 (2000), arXiv:hep-ph/9912253.
- [55] S. Y. Choi, M. Drees, B. Gaissmaier, and J. S. Lee, CP violation in tau slepton pair production at muon colliders, *Phys. Rev. D* **64**, 095009 (2001), arXiv:hep-ph/0103284.
- [56] Y. Li, S. Profumo, and M. Ramsey-Musolf, Higgs-Higgsino-Gaugino Induced Two Loop Electric Dipole Moments, *Phys. Rev. D* **78**, 075009 (2008), arXiv:0806.2693 [hep-ph].
- [57] S. G. Kim, N. Maekawa, A. Matsuzaki, K. Sakurai, and T. Yoshikawa, CP asymmetries of $B \rightarrow \phi K_S$ and $B \rightarrow \eta' K_S$ in SUSY GUT Model with Non-universal Sfermion Masses, *Prog. Theor. Phys.* **121**, 49 (2009), arXiv:0803.4250 [hep-ph].
- [58] S.-G. Kim, N. Maekawa, K. I. Nagao, M. M. Nojiri, and K. Sakurai, LHC signature of supersymmetric models with non-universal sfermion masses, *JHEP* **10**, 005, arXiv:0907.4234 [hep-ph].
- [59] K. Cheung, S. Y. Choi, and J. Song, Impact on the Light Higgsino-LSP Scenario from Physics beyond the Minimal Supersymmetric Standard Model, *Phys. Lett. B* **677**, 54 (2009), arXiv:0903.3175 [hep-ph].
- [60] H. Baer, V. Barger, and P. Huang, Hidden SUSY at the LHC: the light higgsino-world scenario and the role of a lepton collider, *JHEP* **11**, 031, arXiv:1107.5581 [hep-ph].
- [61] K. Sakurai and K. Takayama, Constraint from recent ATLAS results to non-universal sfermion mass models and naturalness, *JHEP* **12**, 063, arXiv:1106.3794 [hep-ph].
- [62] J. Kozaczuk, S. Profumo, M. J. Ramsey-Musolf, and C. L. Wainwright, Supersymmetric Electroweak Baryogenesis Via Resonant Sfermion Sources, *Phys. Rev. D* **86**, 096001 (2012), arXiv:1206.4100 [hep-ph].
- [63] W. Altmannshofer, R. Harnik, and J. Zupan, Low Energy Probes of PeV Scale Sfermions, *JHEP* **11**, 202, arXiv:1308.3653 [hep-ph].
- [64] N. Nagata and S. Shirai, Sfermion Flavor and Proton Decay in High-Scale Supersymmetry, *JHEP* **03**, 049, arXiv:1312.7854 [hep-ph].
- [65] J. S. Kim and T. S. Ray, The higgsino-singlino world at the large hadron collider, *Eur. Phys. J. C* **75**, 40 (2015), arXiv:1405.3700 [hep-ph].
- [66] N. Maekawa, Y. Muramatsu, and Y. Shigekami, Constraints of chromoelectric dipole moments to natural SUSY

- type sfermion spectrum, Phys. Rev. D **95**, 115021 (2017), arXiv:1702.01527 [hep-ph].
- [67] R. Krall and M. Reece, Last Electroweak WIMP Standing: Pseudo-Dirac Higgsino Status and Compact Stars as Future Probes, Chin. Phys. C **42**, 043105 (2018), arXiv:1705.04843 [hep-ph].
- [68] G. Arcadi, A. Djouadi, H.-J. He, J.-L. Kneur, and R.-Q. Xiao, The hMSSM with a light gaugino/higgsino sector: implications for collider and astroparticle physics, JHEP **05**, 095, arXiv:2206.11881 [hep-ph].
- [69] Q. Shafi, A. Tiwari, and C. S. Un, Third family quasi-Yukawa unification: Higgsino dark matter, NLSP gluino, and all that, Phys. Rev. D **108**, 035027 (2023), arXiv:2302.02905 [hep-ph].
- [70] E. Ma, Verifiable radiative seesaw mechanism of neutrino mass and dark matter, Phys. Rev. D **73**, 077301 (2006), arXiv:hep-ph/0601225.
- [71] E. Ma, Common origin of neutrino mass, dark matter, and baryogenesis, Mod. Phys. Lett. A **21**, 1777 (2006), arXiv:hep-ph/0605180.
- [72] D. Hehn and A. Ibarra, A radiative model with a naturally mild neutrino mass hierarchy, Phys. Lett. B **718**, 988 (2013), arXiv:1208.3162 [hep-ph].
- [73] S. Baumholzer, V. Brdar, and P. Schwaller, The New ν MSM ($\nu\nu$ MSM): Radiative Neutrino Masses, keV-Scale Dark Matter and Viable Leptogenesis with sub-TeV New Physics, JHEP **08**, 067, arXiv:1806.06864 [hep-ph].
- [74] S.-L. Chen, A. Dutta Banik, and Z.-K. Liu, Common origin of radiative neutrino mass, dark matter and leptogenesis in scotogenic Georgi-Machacek model, Nucl. Phys. B **966**, 115394 (2021), arXiv:2011.13551 [hep-ph].
- [75] L. Sarma, P. Das, and M. K. Das, Scalar dark matter and leptogenesis in the minimal scotogenic model, Nucl. Phys. B **963**, 115300 (2021), arXiv:2004.13762 [hep-ph].
- [76] D. Mahanta and D. Borah, Fermion dark matter with N_2 leptogenesis in minimal scotogenic model, JCAP **11**, 021, arXiv:1906.03577 [hep-ph].
- [77] D. Borah, P. S. B. Dev, and A. Kumar, TeV scale leptogenesis, inflaton dark matter and neutrino mass in a scotogenic model, Phys. Rev. D **99**, 055012 (2019), arXiv:1810.03645 [hep-ph].
- [78] D. Suematsu, Right-handed neutrino as a common mother of baryon number asymmetry and dark matter, (2024), arXiv:2402.10561 [hep-ph].
- [79] T. Toma and A. Vicente, Lepton Flavor Violation in the Scotogenic Model, JHEP **01**, 160, arXiv:1312.2840 [hep-ph].
- [80] R. L. Workman (Particle Data Group), Review of Particle Physics, PTEP **2022**, 083C01 (2022).
- [81] R. Barbieri, L. J. Hall, and V. S. Rychkov, Improved naturalness with a heavy Higgs: An Alternative road to LHC physics, Phys. Rev. D **74**, 015007 (2006), arXiv:hep-ph/0603188.
- [82] R. Barbieri, M. Frigeni, and G. F. Giudice, Dark Matter Neutralinos in Supergravity Theories, Nucl. Phys. B **313**, 725 (1989).
- [83] J. Aalbers *et al.* (LZ), First Dark Matter Search Results from the LUX-ZEPLIN (LZ) Experiment, Phys. Rev. Lett. **131**, 041002 (2023), arXiv:2207.03764 [hep-ex].
- [84] K. G. Klimenko, Conditions for certain higgs potentials to be bounded below, Theor. Math. Phys.; (United States) **62:1**, 10.1007/BF01034825 (1985).
- [85] G. C. Branco, P. M. Ferreira, L. Lavoura, M. N. Rebelo, M. Sher, and J. P. Silva, Theory and phenomenology of two-Higgs-doublet models, Phys. Rept. **516**, 1 (2012), arXiv:1106.0034 [hep-ph].
- [86] B. Garbrecht and M. Herranen, Effective Theory of Resonant Leptogenesis in the Closed-Time-Path Approach, Nucl. Phys. B **861**, 17 (2012), arXiv:1112.5954 [hep-ph].
- [87] M. Garny, A. Kartavtsev, and A. Hohenegger, Leptogenesis from first principles in the resonant regime, Annals Phys. **328**, 26 (2013), arXiv:1112.6428 [hep-ph].
- [88] M. Beneke, B. Garbrecht, C. Fidler, M. Herranen, and P. Schwaller, Flavoured Leptogenesis in the CTP Formalism, Nucl. Phys. B **843**, 177 (2011), arXiv:1007.4783 [hep-ph].
- [89] M. Beneke, B. Garbrecht, M. Herranen, and P. Schwaller, Finite Number Density Corrections to Leptogenesis, Nucl. Phys. B **838**, 1 (2010), arXiv:1002.1326 [hep-ph].
- [90] W. Buchmuller, P. Di Bari, and M. Plumacher, Leptogenesis for pedestrians, Annals Phys. **315**, 305 (2005), arXiv:hep-ph/0401240.
- [91] J. A. Harvey and M. S. Turner, Cosmological baryon and lepton number in the presence of electroweak fermion number violation, Phys. Rev. D **42**, 3344 (1990).
- [92] D. J. H. Chung, B. Garbrecht, and S. Tulin, The Effect of the Sparticle Mass Spectrum on the Conversion of B-L to B, JCAP **03**, 008, arXiv:0807.2283 [hep-ph].
- [93] N. Aghanim *et al.* (Planck), Planck 2018 results. VI. Cosmological parameters, Astron. Astrophys. **641**, A6 (2020), [Erratum: Astron.Astrophys. 652, C4 (2021)], arXiv:1807.06209 [astro-ph.CO].
- [94] A. Belyaev, G. Cacciapaglia, I. P. Ivanov, F. Rojas-Abatte, and M. Thomas, Anatomy of the Inert Two Higgs Doublet Model in the light of the LHC and non-LHC Dark Matter Searches, Phys. Rev. D **97**, 035011 (2018), arXiv:1612.00511 [hep-ph].
- [95] A. Alloul, N. D. Christensen, C. Degrande, C. Duhr, and B. Fuks, FeynRules 2.0 - A complete toolbox for tree-level phenomenology, Comput. Phys. Commun. **185**, 2250 (2014), arXiv:1310.1921 [hep-ph].
- [96] G. Belanger, F. Boudjema, A. Pukhov, and A. Semenov, micrOMEGAs.3: A program for calculating dark matter observables, Comput. Phys. Commun. **185**, 960 (2014), arXiv:1305.0237 [hep-ph].
- [97] P. Poulose, S. Sahoo, and K. Sridhar, Exploring the Inert Doublet Model through the dijet plus missing transverse energy channel at the LHC, Phys. Lett. B **765**, 300 (2017), arXiv:1604.03045 [hep-ph].
- [98] I. M. Ávila, V. De Romeri, L. Duarte, and J. W. F. Valle, Phenomenology of scotogenic scalar dark matter, Eur. Phys. J. C **80**, 908 (2020), arXiv:1910.08422 [hep-ph].

- [99] A. Belyaev, T. R. Fernandez Perez Tomei, P. G. Mercadante, C. S. Moon, S. Moretti, S. F. Novaes, L. Panizzi, F. Rojas, and M. Thomas, Advancing LHC probes of dark matter from the inert two-Higgs-doublet model with the monojet signal, *Phys. Rev. D* **99**, 015011 (2019), arXiv:1809.00933 [hep-ph].
- [100] J. Kalinowski, W. Kotlarski, T. Robens, D. Sokolowska, and A. F. Zarnecki, Exploring Inert Scalars at CLIC, *JHEP* **07**, 053, arXiv:1811.06952 [hep-ph].
- [101] A. Datta, N. Ganguly, N. Khan, and S. Rakshit, Exploring collider signatures of the inert Higgs doublet model, *Phys. Rev. D* **95**, 015017 (2017), arXiv:1610.00648 [hep-ph].
- [102] A. Ghosh, P. Konar, and S. Seth, Precise probing of the inert Higgs-doublet model at the LHC, *Phys. Rev. D* **105**, 115038 (2022), arXiv:2111.15236 [hep-ph].
- [103] N. Wan, N. Li, B. Zhang, H. Yang, M.-F. Zhao, M. Song, G. Li, and J.-Y. Guo, Searches for Dark Matter via Mono-W Production in Inert Doublet Model at the LHC, *Commun. Theor. Phys.* **69**, 617 (2018).
- [104] B. Dutta, G. Palacio, J. D. Ruiz-Alvarez, and D. Restrepo, Vector Boson Fusion in the Inert Doublet Model, *Phys. Rev. D* **97**, 055045 (2018), arXiv:1709.09796 [hep-ph].
- [105] J. Kalinowski, W. Kotlarski, T. Robens, D. Sokolowska, and A. F. Zarnecki, Benchmarking the Inert Doublet Model for e^+e^- colliders, *JHEP* **12**, 081, arXiv:1809.07712 [hep-ph].
- [106] J. Kalinowski, W. Kotlarski, T. Robens, D. Sokolowska, and A. F. Zarnecki, The Inert Doublet Model at current and future colliders, *J. Phys. Conf. Ser.* **1586**, 012023 (2020), arXiv:1903.04456 [hep-ph].
- [107] K. Avrachenkov, M. Haviv, and P. Howlett, Inversion of analytic matrix functions that are singular at the origin, *SIAM Journal on Matrix Analysis and Applications* **22** (2001).
- [108] M. K. Sain and J. L. Massey, Invertibility of linear time-invariant dynamical systems, *IEEE Transactions on Automatic Control* **14**, 141 (1969).
- [109] T. Hahn, Generating Feynman diagrams and amplitudes with FeynArts 3, *Comput. Phys. Commun.* **140**, 418 (2001), arXiv:hep-ph/0012260.
- [110] V. Shtabovenko, R. Mertig, and F. Orellana, FeynCalc 9.3: New features and improvements, *Comput. Phys. Commun.* **256**, 107478 (2020), arXiv:2001.04407 [hep-ph].
- [111] V. Shtabovenko, R. Mertig, and F. Orellana, New Developments in FeynCalc 9.0, *Comput. Phys. Commun.* **207**, 432 (2016), arXiv:1601.01167 [hep-ph].
- [112] R. Mertig, M. Bohm, and A. Denner, FEYN CALC: Computer algebraic calculation of Feynman amplitudes, *Comput. Phys. Commun.* **64**, 345 (1991).